Nitric oxide donor reveals alterations in interstitial oxygen pressures during skeletal muscle contractions in rats with pulmonary hypertension

by

Kiana Marie Schulze

B.S., Kansas State University, 2019

A THESIS

submitted in partial fulfillment of the requirements for the degree

MASTER OF SCIENCE

Department of Kinesiology
College of Health and Human Sciences

KANSAS STATE UNIVERSITY
Manhattan, Kansas

2020

Approved by:

Major Professor
David C. Poole, D.Sc., Ph.D.

Copyright

Abstract

Introduction: Pulmonary hypertension (PH) is a devastating disease characterized by pulmonary vascular dysfunction and exercise intolerance, due, in part, to gas exchange impediments and impaired cardiac function. In the rat model of PH, we sought to determine whether there are also peripheral (i.e. muscle) aberrations in O_2 delivery-to-utilization matching and vascular control that might contribute to poor exercise tolerance. Furthermore, we investigated peripheral effects of the potent vasodilator, nitric oxide (NO) in attenuating these anticipated decrements.

Methods: Adult male Sprague-Dawley rats were administered a one-time intraperitoneal injection of monocrotaline (MCT; 50 mg/kg) to induce progressive PH. Echocardiography was utilized to monitor disease progression, and at moderate PH preceding right ventricular (RV) failure, experiments were conducted. Phosphorescence quenching protocols determined the partial pressure of O_2 in the interstitial space (PO_2*is*) in the spinotrapezius muscle at rest and during contractions under control (SNP (-)) and NO-donor (SNP (+)) superfusion conditions.

Results: On average, 3-4 weeks post-injection, MCT rats displayed RV hypertrophy (371 ± 46 vs. 251 ± 9 mg), pulmonary congestion, increased right ventricular systolic pressure (48 ± 6 vs. 20 ± 3 mmHg), and arterial hypoxemia (PaO_2: 63.5 ± 3.5 vs. 83.5 ± 3 mmHg) compared to healthy rats ($P \leq 0.05$). No differences were observed in SNP (-) PO_2*is* kinetics or overall muscle oxygenation between healthy and MCT ($P > 0.05$), although PO_2*is* was significantly lower in MCT animals during seconds 10-26 of contractions. SNP (+) unveiled a significantly lower PO_2*is* and overall muscle oxygenation (AUC: 1730 ± 215 vs. 2789 ± 165) throughout contractions in MCT animals versus healthy ($P \leq 0.05$). **Conclusions:** Our findings reveal that, in small muscle mass exercise in MCT rats, muscle oxygenation impairment is significant only during seconds 10-26 after contraction onset and, while NO effectively augments muscle

oxygenation, O_2 delivery-to-utilization matching during contractions is attenuated following increased NO bioavailability in MCT rats. These data support that limitations occurring in whole body exercise, particularly near maximal capacity, may be O_2-delivery-dependent and include impaired NO-mediated vasodilation contributing potentially to a diminished exercise-induced hyperemia and thus exercise intolerance.

Table of Contents

List of Figures

List of Tables

List of Abbreviations

ANOVA	Analysis of Variance
ADMA	Asymmetric dimethylarginine
ADP	Adenosine diphosphate
AT	Acceleration time
ATP	Adenosine triphosphate
AUC	Area under curve
BMPR2	Bone morphogenic protein receptor 2
BW	Body weight
cGMP	Cyclic guanosine monophosphate
CO	Cardiac output
CO_2	Carbon dioxide
DO2	Diffusing capacity
eNOS	Endothelial nitric oxide synthase
ET	Ejection time
ET-1	Endothelin 1
FMD	Flow-mediated dilation
HC	Healthy control
Hct	Hematocrit
HF	Heart failure
HR	Heart rate
HIF-1α	Hypoxia inducible factor 1α
IL-1β	Interleukin-1β

IL-6	Interleukin-6
LV	Left ventricle
MAP	Mean arterial pressure
MCT	Monocrotaline
NIRS	Near infrared spectroscopy
NMD	Nitroglycerin-mediated dilation
NO	Nitric oxide
NOS	Nitric oxide synthase
O_2	Oxygen
$PaCO_2$	Arterial pressure of carbon dioxide
PAH	Pulmonary arterial hypertension
PaO_2	Arterial pressure of oxygen
PAP	Pulmonary arterial pressure
PCr	Phosphocreatine
PDH	Pyruvate dehydrogenase
PDK	Pyruvate dehydrogenase kinase
PGI_2	Prostacyclin
PH	Pulmonary hypertension
Pi	Inorganic phosphate
PO_2	Partial pressure of oxygen
PVR	Pulmonary vascular resistance
$\dot{Q}_m$	Muscle blood flow
$\dot{Q}O_2$	Oxygen delivery

RBC	Red blood cell
ROS	Reactive oxygen species
RV	Right ventricle
RVSP	Right ventricular systolic pressure
SaO_2	Arterial oxygen saturation
sGC	Soluble guanylate cyclase
SNP	Sodium nitroprusside
SV	Stroke volume
TNF-α	Tumor necrosis factor α
TXA_2	Thromboxane A_2
$\dot{V}/\dot{Q}$	Ventilation to perfusion
$\dot{V}_E$	Ventilation
VEGF	Vascular endothelial growth factor
$\dot{V}O_2$	Oxygen utilization
$\dot{V}O_{2max}$	Maximal oxygen uptake
XOR	Xanthine oxidoreductase

Acknowledgements

I would like to acknowledge my mentors Dr. Tim Musch and Dr. David Poole for the opportunity to work in their lab, challenging me to think more deeply, and inspiring my love for research. I also want to thank my committee for their thoughtfulness and dedication to the betterment of their graduate students, Dr. Carl Ade for his patience and assistance, and Sue Hageman for her contribution to surgical preparations. Finally, I acknowledge my lab mates Ramona Weber, Trenton Colburn and Andrew Horn for their support, encouragement, guidance, and willingness to help with studies. It has been a joy and an honor to work with you all.

Dedication

To my parents, Lindel and Myra Schulze, my grandparents, Glenn and Marilyn Wilkens and Arthur and Marjorie Schulze, and my sister, Kiva Schulze. Thank you for your support in all of my endeavors, and your constant encouragement. None of this would have been possible without you.

Chapter 1 - Literature Review

Pulmonary Hypertension

Pulmonary hypertension (PH) is a chronic, progressive disease characterized by a rise in resting pulmonary arterial pressure (PAP) ≥ 20 mmHg and accompanied by exercise intolerance, dyspnea, and reduced quality of life (Simmoneau et al., 2019; Shafazand et al., 2004). There are five groups of etiology, the most severe form being Group 1: pulmonary arterial hypertension (PAH), which is idiopathic in nature, complicating the ability to understand the multifactorial mechanisms underlying this condition (Guignabert & Dorfmüller, 2017). Currently, the median survival time from diagnosis of PAH is 7 years (Benza et al., 2012) and, while the annual prevalence is only 15-26 cases per million, this hinders the ability to perform patient studies and clinical trials (McGoon et al., 2013). Several methods of therapy exist to alleviate symptoms of PH, including endothelin-1 receptor antagonists, prostacyclin infusion and inhalation, and phosphodiesterase-5 inhibitors, all of which target the imbalance between vasoconstricting and vasorelaxing factors within the pulmonary vasculature (Humbert et al., 2004). While some of these treatments have shown beneficial effects such as improvements in exercise capacity, pulmonary hemodynamics, and survivability, they can be expensive, time-intensive, invasive, and elicit adverse effects in some patients (Shafazand et al., 2004). Furthermore, despite alleviating some symptoms of disease, a cure for PH remains to be discovered. Thus, the importance of discerning the pathological mechanisms and sentinel event associated with PAH is paramount.

Central Impairments

Pulmonary Vasculature

The pulmonary vasculature serves an integral purpose to sustaining life as the site of gas exchange between the atmosphere and the body. In health, it receives oxygen (O_2)-depleted blood from all tissues and removes carbon dioxide (CO_2) whilst loading O_2 onto hemoglobin. The arterial endothelium serves a variety of purposes including maintenance of vascular tone, leukocyte trafficking, homeostasis, transduction of luminal signals to abluminal vascular tissues, production of growth factors and cell signals, and serving as a barrier between the lumen and subendothelial layers (Budhiraja et al., 2004). The pathophysiology of PAH still remains elusive, however, there is a widely growing body of literature supporting the notion that endothelial dysfunction in the pulmonary vasculature initiates the cascade of disease (Figure 1). The current hypothesis proposes that endothelial injury triggers apoptosis of typically quiescent endothelial cells, destabilizing the intimal layer, leading to uncontrolled endothelial cell proliferation, and narrowing of the vessel lumen (Budhiraja et al., 2004). Accordingly, a rise in PVR ensues with a concomitant elevation in PAP, thus stimulating mechanical stretch receptors in the endothelium, increasing collagen in the vessel wall and inducing adaptive medial hypertrophy of the vessel (Tozzi et al., 1989). Vascular remodeling continues to narrow the vessel lumen, creating a cycle of increased resistance and pressure. Heightened pressures and endothelial injury create the perfect storm to allow influx of growth factors, fluid, and particulate through the vasculature, which may result in pulmonary congestion and lung edema, reducing diffusing capacity, and impairing gas exchange. This limitation become detrimental as it often leads to hypoxemia and hypercapnia in PH patients, thus increasing respiratory muscle work to regulate blood gases, leading to dyspnea, a hallmark of disease (Babu et al., 2016). Dysregulation of vasoactive

mediators such as increased vasoconstrictors (endothelin-1, ET-1 and thromboxane A_2, TXA_2; Christman et al., 1992; Giaid et al., 1993) and reductions in vasodilators (nitric oxide, NO and prostacyclin, PGI_2; Giaid & Saleh, 1995; Tuder et al., 1999) exacerbate disease progression. Moreover, upregulation of inflammatory cytokines (IL-1β, IL-6, and TNF-α) is thought to further induce vascular dysfunction (Humbert et al., 1995). Decreased NO (Cote et al., 1996), in combination with elevated inflammatory markers and hypoxia (Hassoun et al., 1998), have been shown to stimulate expression of xanthine oxidoreductase (XOR), which contributes to the production of reactive oxygen species (ROS) (i.e., superoxide anion; McCord, 1985). ROS scavenge active NO within the body, thus further attenuating NO levels, exaggerating the vasoconstrictive response of the pulmonary vasculature (Stasch et al., 2011) Whether the dysregulation of vasoactive mediators and inflammatory cytokines occurs as a result of, or coinciding with, endothelial injury has yet to be determined; however, it is currently postulated that the endothelial and vascular dysfunction described herein initiates RV failure seen in PH, which is known to be the primary driver of mortality for patients (Farber et al., 2015; D'Alonzo et al., 1991).

The Right Ventricle

The right ventricle (RV) is the thinner-walled chamber of the heart, equipped to handle high volumes and low pressures. Deoxygenated blood returns from the systemic circulation to the right atrium, where it then flows to the right ventricle to be pumped through the nearby pulmonary circulation. Increased pressures within the pulmonary circulation increase the afterload on this chamber, and, following the Law of LaPlace are thus compensated by increased chamber wall thickness (Bogaard et al., 2009). Sensation by stretch-activated ion channels and

integrins leads to protein synthesis, resulting in sarcomere addition in parallel, increasing myocyte cross sectional area (Mann, 2004; Hu & Sachs, 1997). Compensatory hypertrophy of the RV free wall necessitates elevations in O_2 demand and thus blood flow to supply the tissue. However, in both left ventricular heart failure (LVHF) and monocrotaline (MCT)-induced PH, capillarity is shown to be decreased, which may be related to reduced expression of vascular endothelial growth factor (VEGF), a marker for angiogenesis (Sano et al., 2007; Partovian et al., 1998). When taken together with downregulation of NO, and thus vasodilation, the O_2 delivery-to-demand ratio is disturbed, leading to ischemia, apoptosis, and fibrosis (Kajiya et al., 2007; Tomanek, 1990). As PH progresses, pressures within the RV continue to rise, thus the RV is no longer able to overcome the afterload imposed by the pulmonary vasculature and compensated hypertrophy shifts to RV dilation (sarcomeres added in series), concurrent with contractile impairment (Bogaard et al., 2009). Exercise presents a greater challenge to PH patients because exercise elevates PAPs as well as O_2 demand of the skeletal muscles. Cardiac dysfunction prevents the heart from appropriately increasing stroke volume, and thus cardiac output, reducing O_2 delivery to the periphery, which, in addition to dyspnea culminates in exercise intolerance (Sun et al., 2001).

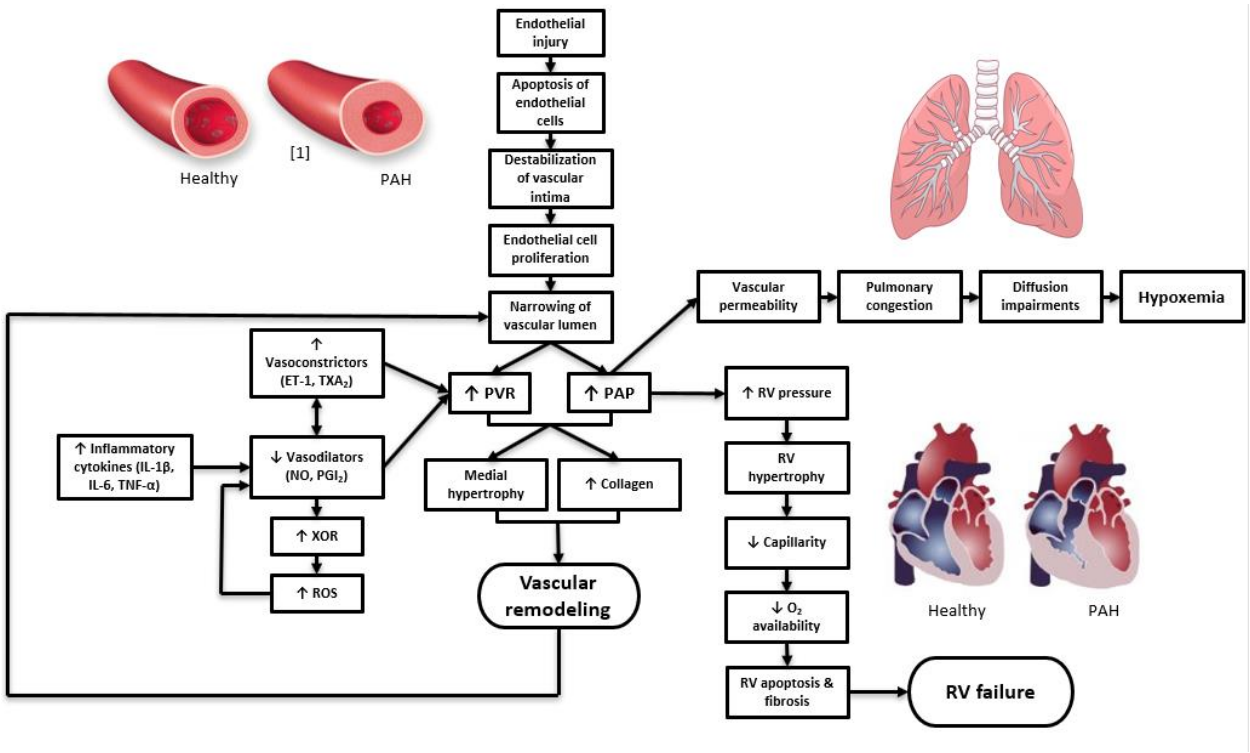

Figure 1: Schematic representation of central impairments in PH. See text for complete explanation of mechanisms. PVR, pulmonary vascular resistance; PAP, pulmonary artery pressure; RV, right ventricle; ET-1, endothelin-1; TXA_2, thromboxane A_2; NO, nitric oxide; PGI_2, prostacyclin; IL-1β, interleukin 1β; IL-6 interleukin 6; TNF-α, tumor necrosis factor-α; XOR, xanthine oxidoreductase; ROS, reactive oxygen species; O_2, oxygen. [1] Rogers et al., 2017.

Peripheral Impairments

In LVHF, the pathology of disease is not attributed to central dysfunction alone, therefore it is suggested that this may manifest in PH patients, as well. Uncertainty remains as to the impact of PH on the periphery, and whether this results from, or accompanies central dysfunction. Specific attention has been paid to skeletal muscle abnormalities and the role of the muscle microcirculation. Within skeletal muscle there is a reduction in cross-sectional area of myocytes, and importantly, a lowered type I to type II fiber ratio, demonstrating that, not only is muscle atrophy apparent, but a greater proportion of muscle may rely upon anaerobic sources of energy production, yielding a much lower adenosine triphosphate (ATP) output per glucose

molecule (Vescovo et al., 1998; Batt et al, 2014). Notably, the increase in type II fibers pertains specifically to type IIb/x, commonly known as the fast-twitch glycolytic fiber type, as opposed to type IIa, which have a greater oxidative capacity (Mainguy et al., 2010). In addition to skeletal muscle alterations, muscle sympathetic nerve activity is heightened in PH patients (Velez-Roa et al., 2004), akin to findings in LVHF where a global sympathetically-mediated vasoconstriction is recognized and exacerbated by sensitization of the exercise pressor reflex (Poole et al., 2011), collectively contributing to a systemic vasoconstrictive response. Vasodilatory capacity has been investigated in response to reactive hyperemia (flow-mediated dilation; FMD) and nitroglycerin-mediated dilation (NMD) (Wolff et al., 2007). Findings suggest endothelial dysfunction as evidenced through decrements in FMD, resulting from impaired shear stress-induced NO release. As stated previously, PH patients display an imbalance in vasoactive mediators in the pulmonary vasculature, namely increases in ET-1 and TXA_2 while reductions are evident in NO and PGI_2. Some evidence suggests that these circulating factors within the plasma may damage the peripheral endothelium as well, further diminishing vasodilatory responses (Klinger et al., 2013). Despite derangements in the NO pathway, nitroglycerin supplementation produced no difference in the vasodilatory response of the peripheral vasculature between healthy and PH patients, thus proposing a role for exogenous NO donation in alleviating vascular dysfunction. Moreover, reduced capillary density (Potus et al., 2014; Mainguy et al., 2010) has been reported in PH patients, which, taken with the diminished vasodilatory response and exaggerated vasoconstriction will compromise skeletal muscle blood flow (Malenfant et al., 2015), and therefore contribute to exercise intolerance.

Exercise

In health, the body adapts to exercise with a wide range of responses, mediated by both central and peripheral factors. Upon exercise onset, the muscle begins contracting, and therefore has increased demands for energy. This energy is utilized in the form of adenosine triphosphate (ATP) which can be synthesized from aerobic and anaerobic metabolism. During intense exercise, or for short durations, ATP is created via the phosphocreatine (PCr) or glycolytic pathways. PCr provides inorganic phosphate (Pi), which combines with adenosine diphosphate (ADP) to yield ATP and creatine (Baker et al., 2010). This reaction can only continue for short periods of time before PCr stores become depleted. Glycolysis utilizes glucose readily available in the blood, or from the breakdown of stored glycogen to produce energy in the cellular cytoplasm, generating 2-3 ATP, respectively, and 2 pyruvate molecules. Pyruvate combines with NADH and H^+ to form lactate and NAD^+, the former of which may accumulate in the muscle, with the latter allowing continuation of glycolysis. In the presence of adequate O_2, pyruvate and NADH can enter the mitochondria to produce ATP via oxidative phosphorylation. With increased exercise duration, energetic demands continue to rise, thus ATP must be synthesized from other sources, and oxidative metabolism increases. Oxidative metabolism allows for the production of 30-33 net ATP, compared to 3 from glycolysis alone. In order for mitochondrial oxidative phosphorylation to occur, there must be sufficient O_2 supply to the muscle, accomplished via increases in skeletal muscle blood flow. Exercise increases sympathetic stimulation while causing vagal withdrawal, augmenting circulating catecholamines such as epinephrine and norepinephrine (Laughlin, 1999). Catecholamines are bound to receptors on the heart, lungs, skeletal muscle, and bodily tissues producing increases in heart rate, vasodilation through the pulmonary circulation and skeletal muscle, and vasoconstriction of renal and

splanchnic regions, collectively resulting in augmented cardiac output, and therefore, oxygen delivery (Laughlin, 1999).

Exercise Intolerance in Pulmonary Hypertension

A hallmark of PH is exercise limitation, demonstrated through reductions in $\dot{V}O_{2peak}$, 6-minute walking distance (6MWD), and muscle force production (Sun et al., 2001; Mainguy et al., 2010). Primary contributions to exercise intolerance in LVHF pertain to aberrations in the O_2 transport pathway, specifically the O_2 delivery ($\dot{Q}O_2$)-O_2 demand ($\dot{V}O_2$) imbalance (Poole et al., 2011). In this regard, PH remains predominantly understudied. At exercise onset, there is a rapid increase in skeletal muscle $\dot{V}O_2$, but in disease states, cardiovascular constraints elicit an insufficient cardiac response to match $\dot{Q}O_2$ to $\dot{V}O_2$, an effect which is exacerbated by endothelial dysfunction and sympathetic nerve overactivation (see *Peripheral Impairments*), subsequently reducing total skeletal muscle oxygenation (Dimopoulos et al., 2013). A paucity of literature exists highlighting $\dot{V}O_2$ uptake kinetics in PH patients. Barbosa et al. demonstrated that PH patients reach a lower $\dot{V}O_{2peak}$, and have a slower kinetic response at the onset of exercise, resulting in a larger O_2 deficit (Barbosa et al., 2011). The consequence of a greater O_2 deficit relates to the metabolic systems supplying energetic demands: a lack of oxygen necessitates reliance upon anaerobic pathways, which produce less ATP, glycogen is depleted, and therefore, they fatigue at much more rapid rates than their oxidative counterparts. Elevated anaerobic metabolism has been further studied by Brown et al. who revealed an increase in glucose transporter GLUT-1 in both the soleus and RV in monocrotaline-treated PH rats (Brown et al., 2015). GLUT-1 is an indicator of cytoplasmic glycolysis, thus heightened levels suggest that glycolysis is amplified in PH. Moreover, PH patients display a preferential shift toward

anaerobic metabolism, a phenomenon paralleled in cancer and termed the "Warburg effect" (Chan & Rubin, 2017). The basis for this shift involves upregulation of hypoxia-inducible factor-1α (HIF-1α) in PH, which generates excessive levels of pyruvate dehydrogenase kinase (PDK). PDK phosphorylates and inhibits the enzyme pyruvate dehydrogenase (PDH) which typically catalyzes the pyruvate to acetyl coenzyme-A reaction; however, when the action of PDH is prevented, pyruvate is instead converted to lactate (Michelakis et al., 2017). Implications of this increased reliance on glycolysis include lactate buildup, supported by occurrence of the lactate threshold at a lower work rate and $\dot{V}O_2$ in PH patients compared with healthy subjects (Mainguy et al., 2010; Batt et al., 2014; Sun et al., 2001). Presumably, these patients are working at a supra-threshold work rate even during normal daily activities, accumulating lactate, thus requiring bicarbonate buffering of hydrogen ions, producing additional CO_2. Increased ventilation is necessary to eliminate this CO_2, and furthermore, hypoxemia may further exaggerate this effect. Sun et al. showed an elevated slope of ventilation ($\dot{V}_E$)/$\dot{V}CO_2$, demonstrating increased work of breathing, confirming that mechanisms beyond cardiopulmonary defects are at work in provoking dyspnea, a major factor in exercise intolerance (Sun et al, 2001).

Summary

Reductions in exercise tolerance are evident in PH patients, and may result from a combination of central and peripheral impairments. Increased pulmonary pressures, further exacerbated by upregulation of vasoconstrictors and reductions in vasodilators, lead to vascular remodeling. Consequently, RV dysfunction arises, potentially diminishing blood flow to the system via contractile and cardiovascular constraint. Reduced blood flow yields tissue hypoxia

which may slow $\dot{V}O_2$ kinetics and, taken with skeletal muscle fiber type alterations and a preference for glycolysis elevate CO_2, supports a peripheral contribution to dyspnea. While these data provide strong evidence for influences on exercise intolerance in patients, they also uncover the need for the mechanistic study of aberrations in the O_2 transport pathway during exercise. Further understanding of these processes may provide fundamental knowledge for designing more effective therapeutic options to improve exercise capacity and quality of life.

Chapter 2 - Introduction

Pulmonary hypertension (PH) is a chronic, progressive disease characterized by hardening of the pulmonary arteries, vascular remodeling, and increased pulmonary arterial pressures (PAP) >20 mmHg at rest (Guignabert & Dorfmüller, 2017; Simonneau et al., 2019). Reduced exercise capacity, and thus quality of life, is a hallmark of PH. The monocrotaline (MCT)-induced pulmonary arterial hypertension rat model has been utilized extensively in animal research. MCT elevates PAPs via endothelial injury and medial hypertrophy of pulmonary vascular smooth muscle (Gomez-Arroyo et al., 2011; Rosenberg & Rabinovitch, 1988). This closely mirrors the symptoms seen in clinical PH (Bogaard et al., 2009), where elevated PAPs increase afterload on the right ventricle (RV), resulting in RV hypertrophy, dilation, and ultimately, RV failure (Gomez-Arroyo et al., 2011). This can lead to decreased stroke volume (SV) at rest and during exercise, and therefore diminished cardiac output (CO), which, in addition to altered pulmonary perfusion distribution, impairs ventilation-perfusion ($\dot{V}/\dot{Q}$) matching, compromising pulmonary gas exchange (especially O_2) and consequently reducing exercise tolerance (Sun et al., 2001; Brown et al., 2015; Babu et al., 2016).

Exercise intolerance has been displayed through attenuations in the 6-minute walking distance (6MWD; Fowler et al., 2011) and quadriceps force production found in humans (Mainguy et al., 2010), as well as a decrease in $\dot{V}O_2max$ in both humans and rats (Brown et al., 2015). Predominantly, scientific investigations have focused on central components of exercise limitations, identifying impairments in the heart, lungs, and respiratory muscles (Sun, 2003; Meyer, 2005; Fowler, 2012; Babu, 2016). $\dot{V}/\dot{Q}$ mismatch is thought to be a primary contributor to the arterial hypoxemia observed in patients (Sun, 2001), likely resulting, in part, from pulmonary edema caused by increased pulmonary pressures and consequent fluid leak. This fluid

thickens the blood-gas barrier, impairing gas exchange across the capillary wall. Alterations in the partial pressure of O_2 and CO_2 in arterial blood (PaO_2 and $PaCO_2$, respectively) stimulate changes in ventilation, which may increase work of breathing and therefore lead to respiratory muscle fatigue, heightening dyspnea. Furthermore, as mentioned above, eventual RV dysfunction may also reduce exercise capacity when considering central limitations to O_2 delivery. Studies directed at peripheral impairments attribute diminutions in exercise capacity to be mediated, in part, by increases in the proportion of Type 2 muscle fibers relative to Type 1 muscle fibers (Mainguy et al., 2010), a shift favoring anaerobic metabolism (Vescovo et al., 1998; Sun et al., 2001; Mainguy et al., 2010), and a decreased gas exchange threshold (Sun et al., 2001; Mainguy et al., 2010). Sithamparanathan et al. have demonstrated that mitochondrial protein levels and enzymatic activity are normal in skeletal muscles of PH patients, suggesting that alterations in oxidative metabolism likely result from a lack of O_2 delivery, rather than dysfunctional mitochondria (Sithamparanathan et al., 2018). The specific role played by the peripheral vasculature and its capacity to augment O_2 flux in response to exercise has yet to be elucidated.

PH is associated with pulmonary vascular dysfunction, specifically within the endothelium in the nitric oxide-soluble guanylate cyclase-cyclic guanosine monophosphate (NO-sGC-cGMP) pathway, where NO levels are attenuated via: a) increased activity of arginase, decreasing L-arginine to NO conversion by means of nitric oxide synthase (NOS), b) increased plasma concentrations of asymmetric dimethylarginine (ADMA), an inhibitor of endothelial NOS (eNOS), c) downregulation or uncoupling of eNOS, or d) inactivation of NO by the superoxide anion (Cella et al., 2001; Stasch et al., 2011).

Near-infrared spectroscopy (NIRS) measurements in PH patients demonstrate decreased tissue oxygenation in skeletal muscle at rest, as well as a slower reactive hyperemia (suggesting impaired flow-mediated vasodilation) compared to both healthy controls and, interestingly, patients with left ventricular heart failure (LVHF) (Dimopoulus et al., 2013). Importantly, NO supplementation via inhaled NO has proven beneficial by enhancing vasodilation in the pulmonary vasculature and decreasing pulmonary vascular resistance (PVR) (Pepke-Zaba et al., 1991; Krasuski et al., 2000). What remains unknown is if this response to NO donors also manifests in increased peripheral (skeletal muscle) O_2 delivery at the level of the capillaries and measured as increased O_2 partial pressure in the interstitial space (i.e. PO_2*is*) in the closest proximity to the contracting myocytes (Hirai et al., 2018).

It has been demonstrated that, in the spinotrapezius muscle of rats with LVHF, there are significant decreases in PO_2*is* when compared with healthy animals (Craig et al., 2019b). Importantly, $PO_2 = \dot{Q}O_2 / \dot{V}O_2$, where $\dot{Q}O_2$ is the delivery of oxygen, which may be limited by a decreased vasodilatory response as a result of endothelial or vascular smooth muscle dysfunction in the skeletal muscle. $\dot{V}O_2$ is oxygen utilization which is dictated by Fick's Law of diffusion: $\dot{V}O_2 = DO_2 \times \Delta PO_2$, where DO_2 is the diffusing capacity at the capillary and ΔPO_2 is the partial pressure gradient of oxygen. A lower resting PO_2*is* therefore suggests a reduced ΔPO_2, decreasing the pressure gradient from the interstitial space into the myocyte, potentially diminishing O_2 that is available to the myocyte, and/or lowering intramyocyte PO_2, thereby altering metabolic control (elevating glycolysis; Hogan et al., 1992). This is indicative of impaired peripheral O_2 delivery-utilization matching.

The objective of this study was to investigate whether the peripheral vasculature (in skeletal muscle) and PO_2*is* kinetics in rats with PH elicit a common pattern to those found

previously in rats with LVHF. Further, we wanted to assess whether the effects of NO supplementation in mitigating the dysfunction seen in the pulmonary vasculature can be translated to the systemic vasculature. We hypothesized that MCT-induced PH rats will exhibit lower resting and contracting PO_2*is* values within the skeletal muscle, and faster PO_2*is* kinetics during the rest-contractions transient than healthy control (HC) rats, indicative of impaired O_2 delivery-utilization matching in the muscle and overall muscle oxygenation, as potential contributors to exercise intolerance. Additionally, we will test the hypothesis that the exogenous NO donor sodium nitroprusside (SNP) will lessen these impairments via a greater vasodilatory response, slowing deoxygenation kinetics and allowing improved muscle oxygenation and therefore muscle function. The results of the present investigation will provide new and unique information concerning the factors that contribute to exercise intolerance found in PH. Finally, the results of these experiments may also provide insight to potential therapeutic modalities that increase NO bioavailability in skeletal muscle in the treatment of this disease.

Chapter 3 - Methods

Animals

All procedures and protocols were approved by the Kansas State University Institutional Animal Care and Use Committee and conducted in accordance with the National Institutes of Health Guide for the Care and Use of Laboratory Animals. Experiments were performed on 21 adult (~2-4 months) male Sprague-Dawley rats (~300 g; Charles River Chicago, Illinois, USA). Upon arrival, animals were maintained in accredited (Association for the Assessment and Accreditation of Laboratory and Animal Care; AAALAC) animal facilities under a 12:12 h light:dark cycle with food and water provided *ad libitum*. Animals were randomized into the MCT-induced PH or healthy control (HC) groups (MCT, n=11, HC, n=10).

Monocrotaline-induced Pulmonary Hypertension

Monocrotaline alkaloid was administered via a one-time intraperitoneal injection at a dosage of 50 mg/kg, which has been shown to produce progressive PH (Mereles et al., 2006; Brown et al., 2015). MCT was dissolved in a solution containing 50% saline and 50% 200-proof ethanol at room temperature and a total of 1 mL of fluid was injected into each rat in the experimental group. HC rats received 1 mL of saline. Significant changes in pulmonary artery pressures, medial thickness of small pulmonary arteries, and RV hypertrophy do not occur until the 3rd or 4th week after MCT exposure, so animals were monitored weekly following injection via echocardiography along with noting body weight and behavioral changes (Lai et al., 1991; Akhavein et al., 2007).

Echocardiography

To ensure adequate development of the disease, transthoracic echocardiography was performed using a commercially available system (Logiq S8; GE Health Care, Milwaukee, WI) with a 13 MHz linear transducer (L4-12t) prior to MCT or saline injection, and then weekly following injection. All comparisons were made between the pre-injection measurement and final measurement taken just prior to experimentation. Animals were initially anaesthetized by inhalation of a 5% isofluorane-O_2 mixture and subsequently maintained on <2.5% isofluorane-O_2 (Butler Health Supply) while positioned on a heating pad to maintain core temperature at ~37°C. 2-D and M-mode images of the left ventricle were obtained from the parasternal short axis window and analyzed for end-systolic/diastolic volumes, stroke volume, and ejection fraction as previously described (Craig et al., 2019a). Right ventricular measurements were taken at the aortic valve in the short axis view just proximal to the pulmonary valve. Pulsed Doppler ultrasound was used to assess pulmonary artery ejection time (ET), acceleration time (AT), and peak velocity, and the ratio of AT to ET (AT/ET) was calculated and used as a clinical parameter for the detection of PH (AT/ET < 0.3; Figure 4; Jones et al., 2002; Kato et al., 2003; Levy et al., 2016). Upon confirmation of PH, the following experiments were performed.

Surgical Preparations

All surgeries were performed utilizing the same anesthetic protocol as described above. Both the right jugular vein and right common carotid artery were surgically isolated and cannulated with a 2-French catheter-tip pressure micromanometer (Millar Instruments, Houston, TX, USA) The micromanometer was advanced into the RV and LV, respectively, to determine pressures within each ventricle. These results were collected using a PowerLab/LabChart data

acquisition system (AD Instruments). After the RV and LV measurements were completed, the micromanometer was withdrawn and right common carotid artery was then catheterized (PE-10 connected to PE-50, Intra-Medic polyethylene tubing; Clay Adams Brand; Becton Dickinson, Sparks, MD) for measurement of mean arterial pressure (MAP) and heart rate (HR) via PowerLab. The caudal artery was surgically isolated and catheterized for administration of pentobarbital sodium. All rats were then progressively transitioned from isoflurane and supplemented with pentobarbital sodium (10mg/kg body weight/hour) as deemed necessary via toe pinch and palpebral reflexes. Incisions were then made to expose the left spinotrapezius muscle, with overlying skin and fascia reflected as previously described (Hirai et al., 2018). Importantly, this preparation does not alter microvascular integrity, or responsiveness of the muscle (Bailey et al., 2000). The spinotrapezius was chosen for its muscle fiber-type composition and citrate synthase activity, which resembles the quadriceps muscle in humans (Delp & Duan, 1996; Leek et al., 2001). Silver wire electrodes were sutured to the rostral (cathode) and caudal (anode) portions of the muscle using 6-0 silk sutures to facilitate electrically-induced twitch contractions. The exposed spinotrapezius was superfused frequently with warmed (38°C) Krebs-Henseleit bicarbonate-buffered solution equilibrated with 5% CO_2-95% N_2 at pH 7.4, and adjacent exposed tissue was covered with Saran Wrap (Dow Brands, Indianapolis, IN) to minimize dehydration.

Experimental Protocol (PO_2)

Following the surgical preparations, the phosphorescent probe Oxyphor G4 (Pd-meso-tetra-(3,5-dicarboxyphenyl)-tetrabenzoporphyrin) was injected into the muscle (~10 µl/injection; 3-4 injections; 10 µM) with care taken to avoid damaging any visible vasculature. After

injection, the muscle was covered with Saran Wrap to protect the muscle from ambient air during a 15-minute period which allows the probe to disseminate throughout the muscle in the interstitial space. The common end of the light guide, of a frequency domain phosphorimeter (PMOD 5000; Oxygen Enterprises, Philadelphia, PA), was positioned ~2-4 mm superficial to the lateral surface of exposed muscle tissue and in a field visibly absent of large vessels. In the first contraction protocol (*hereafter referred to as the SNP (-) condition*), the partial pressure of oxygen in the interstitial space (PO_2*is*) was measured via phosphorescence quenching at rest and during a 180-s contraction protocol (1 Hz, 6 V, 2-ms pulse duration; Grass stimulator model S88, Quincy, MA) and recorded at 2-s intervals (Craig et al., 2019b; Hirai et al., 2018). Dynamic profiles of PO_2*is* during the rest-contraction transition were measured, allowing at least 30-s initially for resting values to be gathered. Following contractions, 20 minutes were allowed for the muscle to fully recover before the experiment was repeated. In the second contraction protocol (*hereafter referred to as the SNP (+) condition*), the spinotrapezius muscle was superfused with the NO donor sodium nitroprusside (SNP; 300μM) before contractions to determine differences between HC and MCT animals in their response to the NO donor. SNP (0.5 mL) diluted in Krebs-Henseleit solution (2.5 mL) was superfused (3 total mL, 1 mL/min) on the muscle for 180-s, followed by a 180-s period of incubation. The light guide remained positioned in the same location as for the first contraction protocol.

Analysis of $PO_2$is Kinetics

The Stern-Volmer relationship was used in calculating PO_2*is*. Direct measurement of phosphorescence lifetime yielded PO_2*is* via the following equation:

$$Po_2 = [\tau_0/\tau - 1] \,/\, (k_Q \; x \; \tau_0)$$

where k_Q is the quenching constant and τ and τ_0 are the phosphorescence lifetimes at the ambient O_2 concentration and in the absence of O_2, respectively. In tissues at 32.3°C (mean spinotrapezius muscle surface temperature was ~33°C), the parameters for G4 are as follows: k_Q of 258 $mmHg^{-1}$ s^{-1} and τ_0 of 226 µs (Esipova et al., 2011). As muscle temperature does not change appreciably during the contraction protocol used herein, the phosphorescence lifetime is determined entirely by the PO_2. The kinetics analyses of the PO_2*is* responses were conducted using 10 s of resting data and the 180-s contraction bout using a monoexponential plus time delay model,

<u>One-component</u>:

$$PO_2(t) = PO_{2(BL)} - \Delta_1 PO_2[1 - e^{-\frac{t-TD}{\tau}}]$$

or a monoexponential plus time delay with a secondary component when necessary

<u>Two component:</u>

$$PO_2(t) = PO_{2(BL)} - \Delta_1 PO_2\left[1 - e^{-\frac{t-TD}{\tau}}\right] + \Delta_2 PO_2[1 - e^{-\frac{t-TD2}{\tau 2}}]$$

where $PO_2(t)$ represents the PO_2*is* at any point in time, $PO_{2(BL)}$ is the baseline PO_2*is* prior to the onset of contractions, Δ_1 and Δ_2 are the amplitudes for the first and second component respectively, TD_1 and TD_2 are the time delays for each component, and τ_1 and τ_2 are the time constants (i.e., the time required to reach 63% of the amplitude) for the primary and secondary amplitudes.

Postmortem Measurements

All rats were euthanized via pentobarbital sodium overdose (>100 mg kg^{-1}, i.a**)**. The RV, LV, lungs, diaphragm, and spinotrapezius muscle, were dissected, extracted and weighed. The right lower leg of each rat was exposed and the tibia bone was isolated, removed, and the length

of the bone was measured. Right ventricular hypertrophy was measured via the Fulton index: RV weight (mg) / LV + septum (S) weight (mg) (Fulton et al., 1952). RV hypertrophy was also expressed as RV/body weight and RV/tibia bone length.

Data and Statistical Analyses

Student paired (within animal) and unpaired (between HC and MCT) t-tests were utilized to determine differences in echocardiographic, morphometric, and pressure measurements, followed by Pearson correlation tests of these data. PO_2*is* dynamic profiles were analyzed via SigmaPlot (Version 14.0) modeling software. A two-way analysis of variance (ANOVA) was used detect differences in PO_2*is* kinetics parameters between the HC and the MCT groups, for both the first (SNP (-)) and second (SNP (+)) contraction protocols. A two-way repeated measures ANOVA assessed interactions in PO_2*is* dynamic profiles.

Chapter 4 - Results

Morphometric Data

Twenty-one animals (HC, n = 10; MCT, n = 11) were analyzed for morphometric and echocardiographic data. Body weight (BW) was significantly lower in the MCT group compared to HC rats upon final measurements (387 ± 13 vs. 451 ± 12 g; $P \leq 0.05$) despite no differences in age upon final measurement, or initial weights. Therefore, RV and lungs were normalized to tibia bone length in addition to BW. Significant increases in RV weight (Figure 2), RV/BW, RV/tibia length, and RV/LV+S were observed in the MCT group compared to HC animals, supporting development of RV hypertrophy/dilation (Table 1). Lung weight, lung/BW, and lung/tibia bone length were all increased in the MCT group compared to HC rats, characteristic of pulmonary congestion (Figure 3; Table 1; Musch, 1993).

Echocardiographic Assessment

There were no differences in any pre-injection measurements between MCT and HC groups. Reductions in PA AT (18 ± 2 vs. 29 ± 1 ms; $P \leq 0.05$), PA peak velocity (81 ± 7 vs. 100 ± 5 cm/s; $P \leq 0.05$), and the AT/ET ratio (0.22 ± 0.02 vs. 0.35 ± 0.01 ms; $P \leq 0.05$) were present during the final echocardiographic measurement of MCT rats versus the final measurement of HC animals (Figure 4; Table 2). MCT animals also experienced attenuations in PA AT (18 ± 2 vs. 29 ± 2 ms; $P \leq 0.05$) and AT/ET (0.22 ± 0.02 vs. 0.34 ± 0.02; $P \leq 0.05$) when compared to pre-injection measurements. There were no differences in pre-injection left ventricular measurements between MCT and HC groups; however, HC rats displayed an increase in stroke volume from pre-injection to final measurement (0.58 ± 0.06 vs. 0.75 ± 0.05 mL; $P \leq 0.05$),

while MCT rats did not (0.51 ± 0.05 vs. 0.53 ± 0.06; $P > 0.05$). No other changes in left ventricular measurements were apparent between the two groups at final assessment. Right ventricular systolic pressure (RVSP) was augmented in the MCT group compared to HC (48 ± 6 vs. 20 ± 3 mmHg; $P \leq 0.05$). RVSP was negatively correlated with AT/ET, suggestive of increased afterload yielding elevated systolic pressures within the RV (Figure 5).

Phosphorescence Quenching ($PO_2$is)

Sixteen rats were utilized for SNP (-) PO_2 measurements due to five animals not completing the protocol (HC n = 9; MCT n = 7), with one rat not completing the SNP (+) protocol (HC n = 9; MCT n = 6). Resting MAP and HR did not differ between HC and MCT groups in either the SNP (-) (103 ± 2 vs 95 ± 3 mmHg; 361 ± 8 vs. 390 ± 13 bpm; $P > 0.05$) or the SNP (+) condition (106 ± 6 vs. 96 ± 5 mmHg; 349 ± 8 vs. 378 ± 13 bpm; $P > 0.05$). MAP and HR did not change significantly during the contraction protocol in HC or MCT rats during either condition, and did not differ between groups. Arterial blood gas samples, taken immediately following the SNP (-) contraction protocol, displayed no differences in pH, lactate concentration ($[La^-]$), hematocrit (Hct), or $PaCO_2$ between groups ($P > 0.05$; Table 3); however, significant decreases were observed for PaO_2 and SaO_2 in MCT rats in these samples ($P \leq 0.05$; Table 3).

Group mean PO_2*is* profiles at rest and during contractions in both conditions are presented in Figure 6. There were no significant differences in the kinetics parameters between HC and MCT groups during SNP (-) contractions ($P > 0.05$; Table 4). Despite this, during seconds 10-26 of SNP (-) contractions, PO_2*is* values were significantly reduced in MCT animals ($P \leq 0.05$; Figure 6A). SNP (+) contractions exhibited elevated $PO_2is_{(BL)}$, PO_2is_{nadir}, Δ_1, and area

under the curve (AUC) in both groups compared to SNP (-) ($P \leq 0.05$; Table 4). Although no significant differences were observed in the response to SNP superfusion (i.e.; ΔPO_2is, τ, AUC) between groups (Figure 7; Table 5), PO_2is values (Figure 6B; Table 6), as well as AUC (i.e., overall muscle oxygenation) were significantly lower in MCT rats during SNP (+) contractions versus HC rats ($P \leq 0.05$; Figure 8; Table 4). Taken with faster kinetics (i.e., τ; Table 4) in MCT animals compared to HC rats during SNP (+) contractions, this suggests that despite positive effects of SNP on overall muscle oxygenation in MCT rats, impairments are still present compared to HC animals.

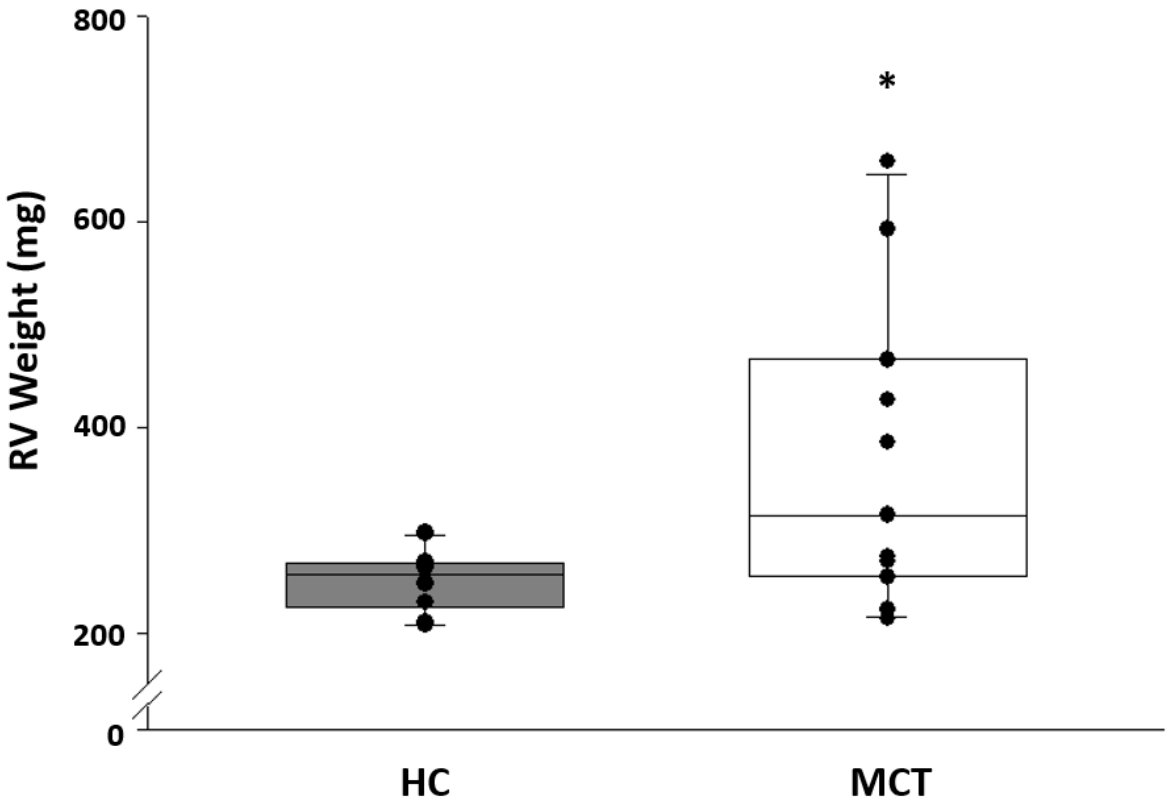

Figure 2: Absolute values for right ventricular weight in healthy (HC, n = 10) and MCT-treated (n = 11) rats. Box plots indicate 10^{th}, 25^{th}, 50^{th}, 75^{th}, and 90^{th} percentile of group data. Individual values plotted. Analyzed via unpaired student's t-tests. * $P \leq 0.05$ vs. healthy

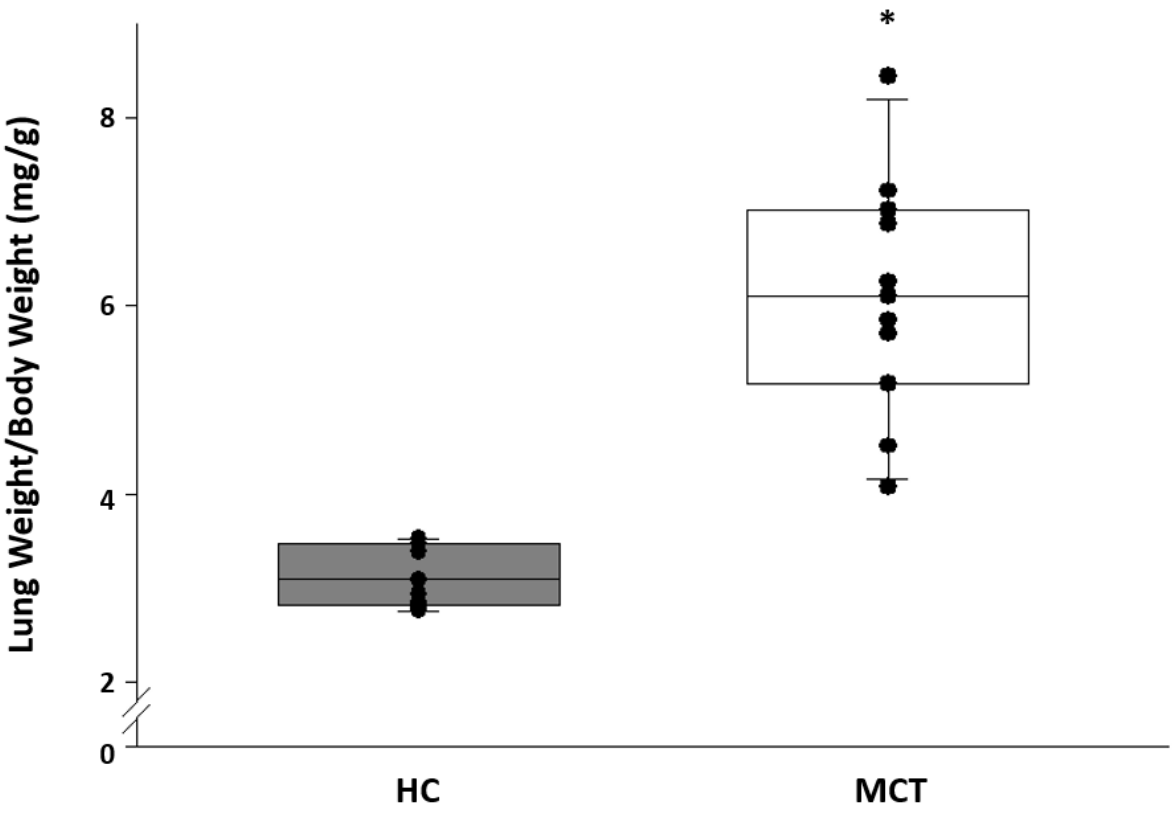

Figure 3: Relative values for lung weight corrected for body mass in healthy (n = 10) and MCT (n = 11) rats. Analyzed via unpaired student's t-tests. * $P \leq 0.05$ vs. healthy

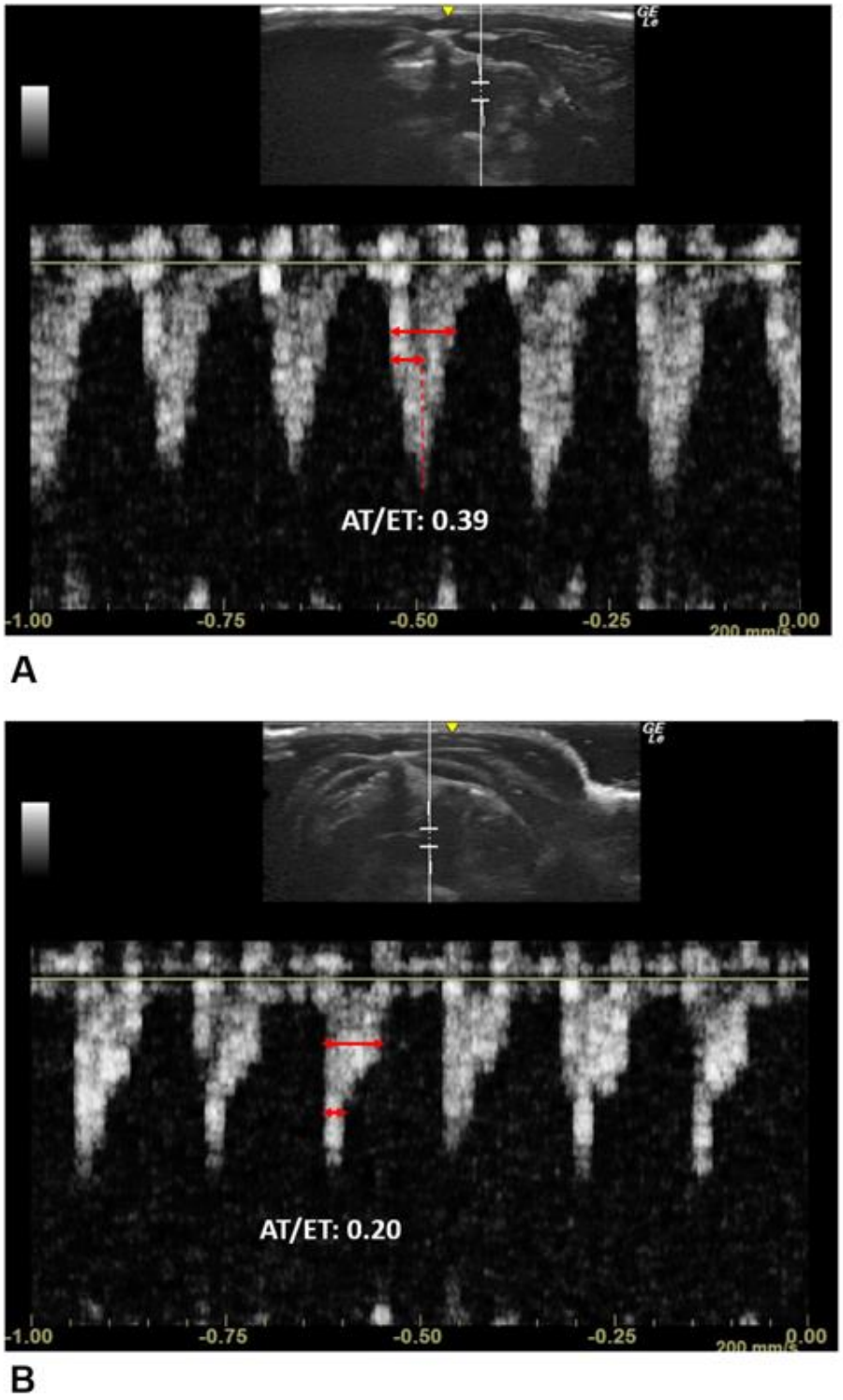

Figure 4: Representative echocardiographic Doppler images and corresponding values for ratio of acceleration time to ejection time in healthy **(A)** and MCT **(B)** rats at final measurement. Top panel indicates measurement taken at level of pulmonary artery. Arrows indicate ejection time (ET; top arrow) and acceleration time (AT; lower arrow). Dashed line indicates end of AT (at peak velocity) for clarity.

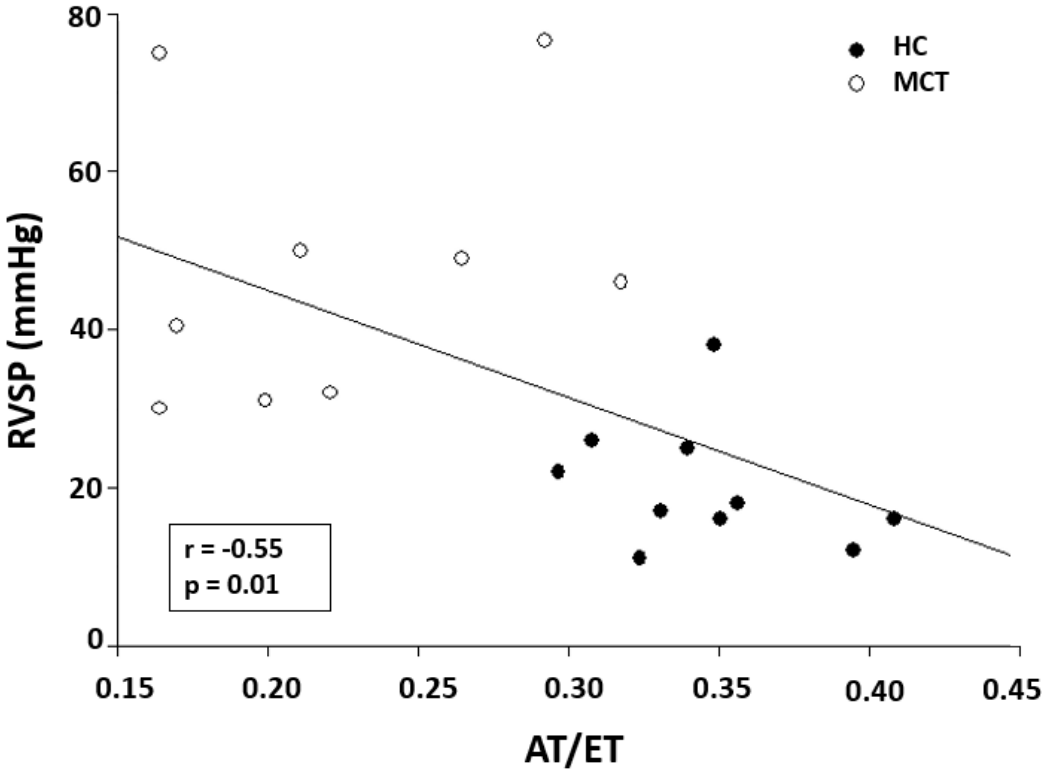

Figure 5: Linear regression showing correlation between right ventricular systolic pressure (RVSP) and AT/ET ratio in HC (n = 10) and MCT (n = 9) rats.

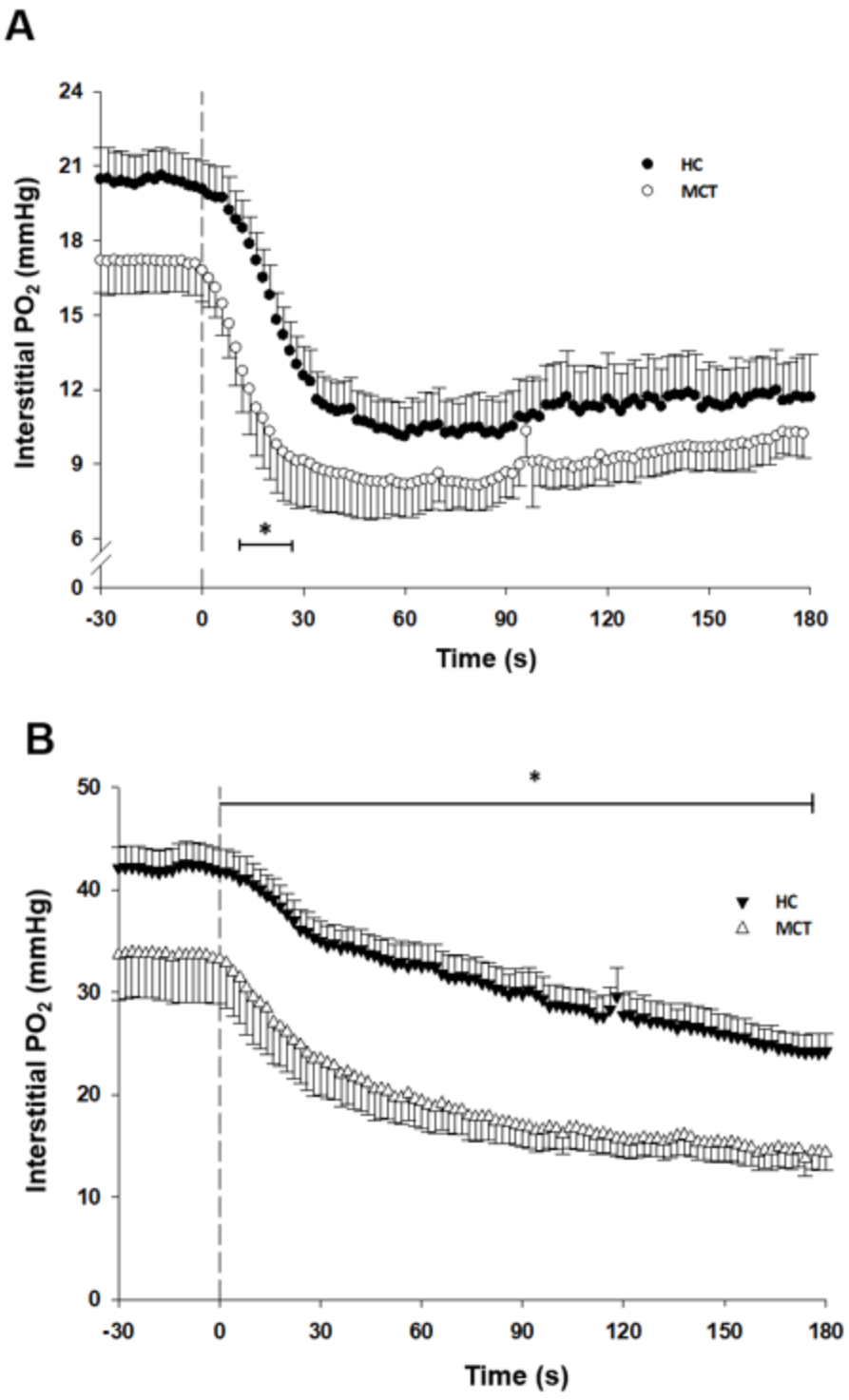

Figure 6: Group mean PO_2*is* dynamic profiles during 30 seconds of rest and 180 seconds of contractions. Dashed line indicates onset of contractions. Analyzed via two-way repeated measures ANOVA. * $P \leq 0.05$ between mean HC and MCT PO_2*is* values for all timepoints included (SNP (-), 10-26s; SNP (+) 0-180s). **A)** SNP (-) condition (HC, n = 9; MCT, n = 7). **B)** SNP (+) condition (HC, n = 9; MCT, n = 6).

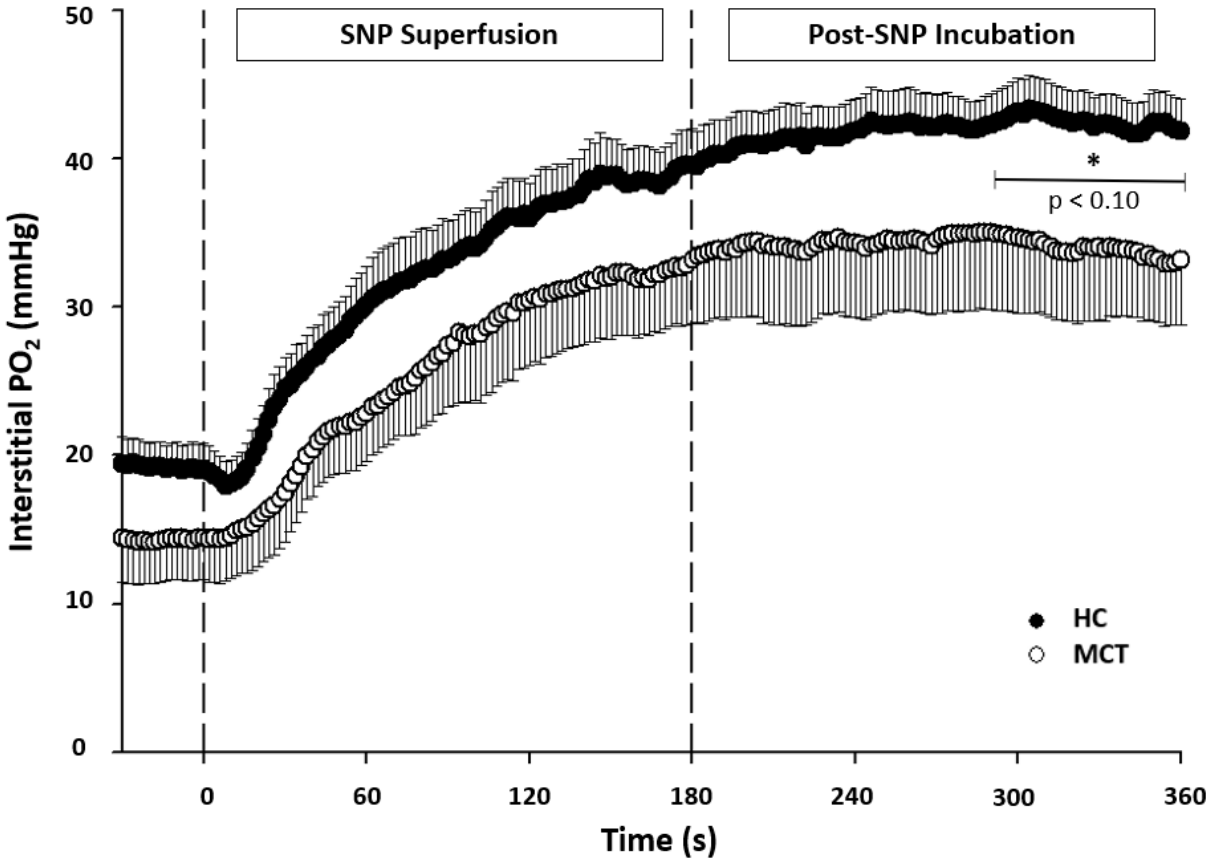

Figure 7: Group mean PO_2*is* profiles for resting (30 s), SNP superfusion (180 s) and incubation (180 s) in healthy (n = 9) and MCT (n = 6) rats. Dashed lines indicate onset (0 s) and termination (180 s) of superfusion. Analyzed via two-way repeated measures ANOVA. * P < 0.10 vs. healthy PO_2*is* values at all given timepoints (292-360 s).

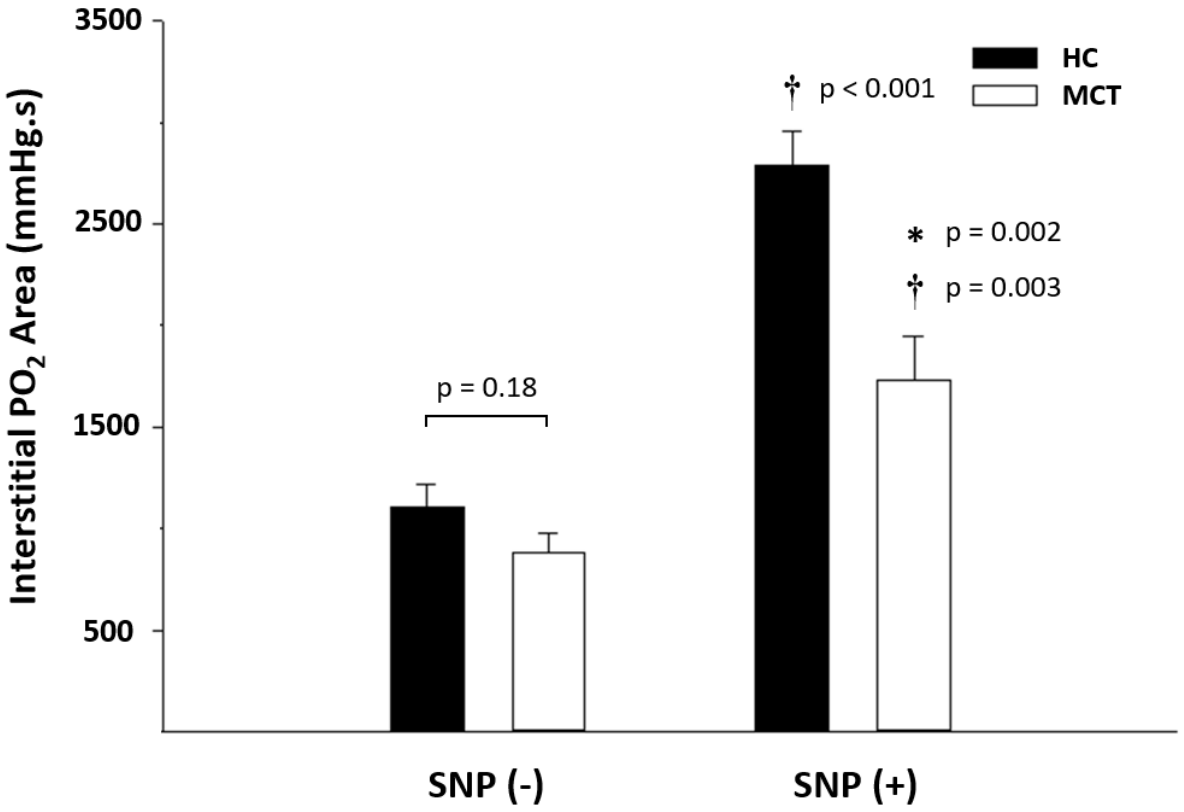

Figure 8: Mean area under the curve for 180 s of contractions in SNP (-) (HC, n = 9; MCT, n = 7) and SNP (+) conditions (HC, n = 9; MCT, n = 6). Analyzed via two-way ANOVA. * $P \leq 0.05$ vs. healthy rats within condition; † $P \leq 0.05$ vs. SNP (-) within group.

Table 1: Morphometric data. Values are means ± SE. Healthy (n = 10), MCT (n = 11). RV, right ventricle; LV + S, left ventricle plus septum; RA, right atrium; LA, left atrium; BW, body weight; Tibia, tibia bone length. Analyzed via unpaired student's t-test. * $P \leq 0.05$ vs. healthy

	Healthy	MCT
RV (mg)	251 ± 9	371 ± 46 *
LV+S (mg)	900 ± 38	832 ± 40
Lungs (mg)	1403 ± 73	2354 ± 154 *
Diaphragm (mg)	987 ± 44	944 ± 51
RA (mg)	46 ± 5	78 ± 23
LA (mg)	36 ± 4	27 ± 1
RV/LV+S (mg/mg)	0.28 ± 0.01	0.44 ± 0.04 *
Lung/BW (mg/g)	3.14 ± 0.11	6.11 ± 0.38 *
Lung/Tibia (mg/mm)	32.7 ± 1.6	55.0 ± 4.7 *
RV/BW (mg/g)	0.56 ± 0.02	0.95 ± 0.10 *
RV/Tibia (mg/mm)	6.0 ± 0.2	8.3 ± 1.1 *
Body Wt (g)	451 ± 12	387 ± 13 *

Table 2: Echocardiographic measurements. Values are means ± SE. Healthy (n = 10), MCT (n = 11). RVSP, right ventricular systolic pressure. Analyzed via paired and unpaired student's t-test. * $P \leq 0.05$ vs. healthy, † $P \leq 0.05$ vs. pre-injection within group.

	Healthy		MCT	
	Pre	Final	Pre	Final
Ejection Time (ET) (ms)	87 ± 3	83 ± 2	84 ± 3	84 ± 3
Acceleration Time (AT) (ms)	32 ± 2	29 ± 1	29 ± 2	18 ± 2 † *
Peak Velocity (cm/s)	90 ± 7	100 ± 5	89 ± 4	81 ± 7 *
AT/ET	0.37 ± 0.03	0.35 ± 0.01	0.34 ± 0.02	0.22 ± 0.02 † *
RVSP (mmHg)		20 ± 3		48 ± 6 *

Table 3: Blood gas values. Values are means ± SE. Healthy (n = 9), MCT (n = 7). Hct, hematocrit. Analyzed via unpaired student's t-test. * $P \leq 0.05$ vs. healthy.

	Healthy	MCT
pH	7.4 ± 0.1	7.4 ± 0.0
PCO_2 (mmHg)	31.1 ± 1.1	30.6 ± 1.7
PO_2 (mmHg)	83.5 ± 3.0	63.5 ± 3.5 *
% O_2 Sat	95.0 ± 1.0	88.6 ± 2.2 *
Hct (%)	33.0 ± 1.1	32.1 ± 1.3
Lactate (mmol/L)	1.0 ± 0.1	1.0 ± 0.1
Bicarbonate (mmol/L)	21.0 ± 0.4	20.7 ± 0.8
Base Excess (mmol/L)	-3.5 ± 0.5	-3.7 ± 0.8
Total CO_2 (mmol/L)	21.9 ± 0.4	21.7 ± 0.9

Table 4: Interstitial PO_2 kinetics parameters of spinotrapezius at rest and during 180 s of contractions in SNP (-) condition and following SNP superfusion. Values are means ± SE. SNP (-) (healthy, n = 9; MCT, n = 7), SNP (+) (healthy, n = 9; MCT n = 6). $PO_2is_{(BL)}$, baseline interstitial PO_2; PO_2is_{nadir}, nadir of PO_2 profile; Δ_1, PO_2 primary amplitude; PO_2is_{end}, interstitial PO_2 at end-contractions; τ, time constant; PO_2 at τ, interstitial PO_2 value at timepoint of τ; AUC, area under the curve. Analyzed via two-way ANOVA. * $P \leq 0.05$ vs. healthy within condition, † $P \leq 0.05$ vs. SNP (-) within group.

	SNP (-)		SNP (+)	
	Healthy	MCT	Healthy	MCT
$PO_2is_{(BL)}$ (mmHg)	20.8 ± 2.0	17.1 ± 1.2	42.2 ± 2.2 †	33.5 ± 4.5 † *
PO_2is_{nadir} (mmHg)	9.9 ± 1.6	7.4 ± 1.0	24.5 ± 2.0 †	14.2 ± 1.7 † *
Δ_1 (mmHg)	10.9 ± 1.1	9.7 ± 0.8	17.6 ± 1.7 †	19.4 ± 3.3 †
PO_2is_{end} (mmHg)	12.6 ± 1.9	10.2 ± 0.9	24.3 ± 1.7 †	14.4 ± 1.8 *
τ (s)	24.1 ± 2.5	22.1 ± 5.6	64.1 ± 9.4 †	41.0 ± 10.7 *
PO_2 at τ (mmHg)	14.0 ± 1.7	11.0 ± 1.0	31.1 ± 1.9 †	21.3 ± 2.6 † *
AUC	1103 ± 115	884 ± 95	2789 ± 165 †	1730 ± 215 † *

Table 5: Interstitial PO_2 kinetics parameters of spinotrapezius at rest and during 180 s of SNP superfusion and subsequent 180 s of incubation. Values are means ± SE. Healthy (n = 9), MCT (n = 6). Resting PO_2*is*, interstitial PO_2 in resting muscle prior to SNP superfusion; PO_2is_{nadir}, nadir of PO_2 profile; ΔPO_2*is*, amplitude of rise in PO_2 throughout SNP superfusion and incubation; End PO_2, interstitial PO_2 at end of SNP incubation; τ, time constant; PO_2 at τ, interstitial PO_2 value at timepoint of τ; AUC, area under the curve. Analyzed via unpaired student's t-test.

	Healthy	MCT
Resting PO_2 (mmHg)	19.1 ± 1.7	14.4 ± 2.8
ΔPO_2*is* (mmHg)	23.1 ± 2.0	19.2 ± 3.6
End PO_2 (mmHg)	42.2 ± 2.2	33.5 ± 4.5
τ (s)	104.6 ± 13.4	92.7 ± 16.1
PO_2 at τ (mmHg)	33.6 ± 1.8	26.4 ± 3.6
AUC	6941 ± 381	5615 ± 756

Table 6: Group mean PO_2*is* values at given timepoints throughout 180 s of contractions. Values are means ± SE. SNP (-) (healthy n = 9; MCT, n = 7), SNP (+) (healthy, n = 9; MCT, n = 6). Δ, difference between SNP (+) PO_2*is* value and SNP (-) PO_2*is* value at given timepoint. Analyzed via paired and unpaired student's t-test. * $P \leq 0.05$ vs. healthy within condition, † $P \leq 0.05$ vs. SNP (-) within group.

	SNP (-)		SNP (+)		Δ	
	Healthy	MCT	Healthy	MCT	Healthy	MCT
0 s (BL)	20.1 ± 1.1	17.3 ± 1.5	41.8 ± 2.2 †	33.2 ± 4.4 † *	21.7 ± 1.6	16.0 ± 4.3
10 s	19.1 ± 1.9	14.7 ± 1.8	40.5 ± 2.1 †	29.5 ± 4.6 † *	21.4 ± 1.9	14.8 ± 4.3
20 s	15.9 ± 1.8	10.9 ± 2.3	37.7 ± 2.0 †	26.1 ± 3.9 † *	21.8 ± 1.6	15.2 ± 3.9
30 s	12.5 ± 1.5	9.1 ± 2.2	35.0 ± 1.9 †	23.5 ± 3.5 † *	22.5 ± 1.5	14.4 ± 3.6 *
60 s	10.4 ± 1.6	8.2 ± 1.6	32.6 ± 2.0 †	19.3 ± 2.7 † *	22.2 ± 2.1	11.1 ± 2.6 *
90 s	11.0 ± 1.7	8.5 ± 1.2	29.9 ± 2.1 †	17.0 ± 2.1 † *	18.9 ± 2.0	8.4 ± 1.7 *
120 s	11.7 ± 2.0	9.5 ± 1.2	27.8 ± 2.1 †	15.7 ± 1.8 † *	16.1 ± 2.0	6.2 ± 1.3 *
150 s	12.2 ± 1.8	9.9 ± 1.0	26.0 ± 1.9 †	15.2 ± 1.8 † *	13.8 ± 2.1	5.3 ± 1.1 *
180 s	12.7 ± 1.9	10.5 ± 1.2	24.4 ± 1.6 †	14.4 ± 1.7 † *	11.8 ± 2.1	3.9 ± 0.9 *

Chapter 5 - Discussion

The primary original findings of this investigation support that the kinetics of $\dot{Q}O_2$-to-$\dot{V}O_2$ matching are not impaired at rest or during submaximal muscle contractions in MCT-induced PH rats. Importantly, significant decrements are present in MCT rats during that crucial window following the onset of contractions. Additionally, increasing NO bioavailability via the exogenous NO-donor SNP improved skeletal muscle oxygenation in this model of PH, similar to HC animals; however, these improvements were diminished during contractions following NO supplementation compared to HC rats. These results partially support our hypothesis that MCT rats elicit decrements in PO_2*is* during exercise compared to HC animals; although, contrary to our hypothesis, these effects were observed only during the SNP (+) condition. This suggests that peripheral vasculature dysfunction is present in MCT-induced PH, however, it is not revealed in single-muscle submaximal exercise, alone. It is pertinent that this dysfunction may become apparent when a larger proportion of skeletal muscle is recruited, such as in whole body exercise. These findings are paramount to understanding the mechanisms associated with impaired exercise capacity in PH patients by demonstrating that they can sustain small-muscle mass submaximal exercise without experiencing O_2 transport-related decrements in O_2 delivery-demand matching. It also offers a potential window into the design of therapeutic rehabilitation modalities that will be well tolerated.

The MCT model allows mechanistic study of PH and has reliably demonstrated increases in RVSP (Chesney et al., 1974), RV weight (Chesney et al., 1974; Meyrick et al., 1980; Jones et al., 2002; Kato et al., 2003), and decreases in PA AT and AT/ET (Jones et al., 2002; Kato et al., 2003), consistent with the pathology of PH patients (Kitabatake et al., 1983; Velez-Roa et al., 2004, Bogaard et al., 2009). Tables 1 and 2 demonstrate that the animals in the present

investigation experienced these impairments within 3-4 weeks post-injection. A prominent clinical hallmark of patients with PH is chronic hypoxemia at rest and during exercise (Rich et al., 1987; Hoeper et al., 2007), purportedly related to $\dot{V}/\dot{Q}$ mismatch, or diffusion limitations as evidenced through lowered DL_{CO} (Rich et al., 1987; Sun et al., 2003; Meyer et al., 2005; Barbosa et al., 2011). Given that $PaCO_2$ is unchanged herein, it is noteworthy that $PaCO_2$ is more tightly regulated than PaO_2 due to the difference in the shape of their dissociation curves and sensitivity of chemoreceptors to small changes in $PaCO_2$ (West, 2012). Thus, CO_2 will be predominantly defended in the event of inefficient gas exchange, therefore indicating a prospective cause for hypoxemia in the absence of hypercapnia in our investigation (Table 3).

Pulmonary Hypertension and Interstitial PO_2

Preservation of PO_2*is* in the face of attenuated PaO_2 and SaO_2 requires compensation in $\dot{Q}O_2$ or $\dot{V}O_2$ in the SNP (-) condition (Figure 6). Importantly, $PO_2 = \dot{Q}O_2/ \dot{V}O_2$, where $\dot{Q}O_2$ is oxygen delivery, which is determined by $\dot{Q}_m$ x CaO_2 where $\dot{Q}_m$ is blood flow to the muscle and CaO_2 is the content of oxygen in the arterial blood. Since $CaO_2 = ([Hb] \times 1.34 \times SaO_2) + (PaO_2 \times 0.003)$, unaltered Hct and thus [Hb] between HC and MCT rats herein (Table 3) indicate that a fall in PaO_2, and thus SaO_2, would cause a reduced CaO_2, and a consequent drop in $\dot{Q}O_2$. Therefore, to maintain PO_2*is* at the same level as HC animals, either $\dot{V}O_2$ must be lowered to the same degree as $\dot{Q}O_2$, or $\dot{Q}_m$ must be elevated. It is doubtful that $\dot{V}O_2$ is decreased, as the electrical stimulation for muscle contractions is the same across all animals (6 V, 1 Hz, 180 s), and therefore oxygen demands on the muscle are considered to be equivalent, which, taken with unchanged function of mitochondria (i.e., O_2 utilization; Sithamparanathan et al., 2018) suggests that, in order to provide adequate oxygen, $\dot{Q}O_2$ must be increased via augmentation of $\dot{Q}_m$. This

compensatory mechanism would allow the muscle to meet O_2 demands during exercise, at least in this acute, small muscle, submaximal condition.

During high-intensity exercise in PH patients, $\dot{V}O_2$ kinetics are slowed, likely due, in part, to O_2 delivery limitations, as indicated by the more rapid kinetics and greater amplitude of muscle fractional O_2 extraction relative to $\dot{V}O_2$ (Barbosa et al., 2011). These findings appear contrary to our observations that $\dot{Q}_m$ may have been augmented and the PO_2 (inversely related to fractional O_2 extraction) was unchanged between HC and MCT animals. Notably, during seconds 10-26 during SNP (-) contractions, PO_2*is* values of MCT rats were lower than those of their healthy counterparts. Despite no differences in the overall PO_2*is* kinetics, the lower PO_2*is* at that time when the mitochondria are trying to increase $\dot{V}O_2$ and ATP production most rapidly may contribute to an impairment of $\dot{V}O_2$ kinetics. Furthermore, whole body exercise necessitates the redistribution of blood flow to accommodate O_2 delivery-demand matching of additionally recruited muscle mass. Therefore, the discrepancy may be explained by the contrast between the systemic demands of whole body versus single muscle exercise seen herein. The slowing of $\dot{V}O_2$ kinetics during exercise produces an increased O_2 deficit, and thus greater reliance upon anaerobic pathways for ATP regeneration, thereby increasing production of metabolic by-products (Poole et al., 2008). Accordingly, this leads to a lactic acidosis, attended by muscle fatigue and production of excess CO_2, further stimulating ventilatory drive. Similarly, findings of an elevated $\dot{V}_E/\dot{V}CO_2$ slope during exercise indicate a higher work of breathing (Sun et al., 2001), promoting dyspnea, escalating the work of the diaphragm, and potentially accompanied by respiratory muscle cardiac output steal (Harms et al., 1997). This redistribution of blood flow from the working locomotor muscles, in addition to, or concomitant with, potential sympathetic nervous activation (Velez-Roa et al., 2004) and endothelial dysfunction (Wolff et al., 2007;

Peled et al., 2008) is expected to contribute to exercise intolerance seen in whole body exercise in PH patients.

Interstitial PO_2 with NO Donor

Upon superfusion of the NO-donor SNP, the vasodilatory response occurs in a commensurate manner to that of HC animals, as evidenced by unchanged AUC, ΔPO_2*is*, t_{63} and PO_2*is* levels during and following superfusion (Figure 7; Table 5). However, during SNP (+) contractions, the PO_2*is* is lowered in MCT animals (Figure 6; Table 6). In the event that MCT animals were already compensating for hypoxemia by elevating muscle blood flow in the SNP (-) condition, it is possible that there is a ceiling effect, where the SNP presumably causes the vasculature approximate its maximal vasodilatory capacity. This may be a result of thickening and hardening of vessels leading to vascular constraint, or due to increased vasomotor tone attributable to upregulation of vasoconstrictors such as endothelin-1 (ET-1) and thromboxane A_2 (TXA_2) and downregulation of PGI_2 and endogenous NO, which has been observed in the pulmonary vasculature, and may also be present in the periphery (Budhiraja et al., 2004). Therefore, upon start of contractions, further arteriolar dilation is constrained and no longer able to further increase blood flow and O_2 delivery, thus lowering PO_2*is*, whereas HC animals still have the capacity to allow for enhanced blood flow. Wolff et. al. have shown that, in patient populations comparing NO-induced vasodilation with flow-mediated dilation (FMD) at rest via brachial artery occlusion and reperfusion, the NO donor allowed for similar increases in vasodilatory capacity as HC animals; however, in FMD, there are significant attenuations in the vasodilatory response (Wolff et al., 2007). This is consistent with our findings that the resting muscle vasodilatory response to NO was unchanged between HC and MCT animals and raises

the question of whether the greater decreases seen in PO_2*is* and faster τ during SNP (+) are a result of an impaired endothelial response to exercise-induced hyperemia. Similarly, studies have shown that peripheral endothelial dysfunction is positively correlated with disease severity, exercise intolerance via 6MWD, and pulmonary pressure in patients, which may provide direction for future investigation of the endothelium, specifically, in isolated peripheral vessel responses to flow and vasoactive mediators (Peled et al., 2008).

Clinical Implications

The importance of PO_2*is* preservation during single-muscle contractions in MCT-induced PH is underscored by findings which illustrate that small muscle exercise training is feasible and can improve a cardiovascular (heart failure with reduced ejection fraction; HFrEF) patient's ability to perform whole body exercise (Esposito et al., 2011). In whole body exercise it is likely that $\dot{V}/\dot{Q}$ mismatch heightens diaphragm activity to increase ventilation, contributing to respiratory muscles stealing blood flow from the locomotory muscles (Harms et al., 1997), yielding dyspnea as well as exhaustion. This phenomenon has been reported in other pathologic states such as LVHF (Musch, 1993; Olson et al., 2010) and chronic obstructive pulmonary disease (Borghi-Silva et al., 2008). Should single muscle, or at least small muscle mass exercise improve the capacity for whole body exercise, alleviating effects of respiratory muscle steal and improving overall exercise capacity, this finding would be relevant to designing exercise therapy regimens, considering the beneficial effects of exercise training on PH. Brown et al. have found that both acute and chronic exercise training has proven beneficial in alleviating symptoms of PH such as elevated RVSP and PAP, and markers of RV hypertrophy including RV free wall thickness, RV to LV + S ratio, and fibrotic indicators such as apelin in MCT-treated rats (Brown

et al., 2015, 2017). Furthermore, exercise training in PH patients improves their exercise capacity that is associated with improvements in 6MWD, $\dot{V}O_2$peak (Grünig et al., 2011), muscle capillarity (i.e.; O_2 delivery), gas exchange threshold, quadricep strength, and time to exhaustion in exercise tests (de Man et al., 2009). Taken together, these data suggest that small muscle mass exercise may be tolerated in these patients, and restore their ability to participate in whole body exercise, which may prove to be a noteworthy therapeutic strategy for lessening symptoms of disease, as well as improving quality of life (Mereles et al., 2006; Grünig et al., 2011).

Experimental Considerations

While this study focused only on male animals, human females exhibit a higher incidence of PH, however, they also display better outcomes (i.e. survivability) than males (McGoon et al., 2013; Lahm et al., 2014), therefore future studies should investigate female and female ovariectomized rats to understand the effects estrogen may play in skeletal muscle vascular function within this disease. It is also worth considering that the MCT-induced PH model, while commonly used (Ryan et al., 2013; Nogueira-Ferreira et al., 2015) may be exhibiting so far undetermined peripheral effects which may confound data interpretation: Being a result of MCT, not PH per se. While this is possible, MCT is metabolized in the liver and bound to red blood cells (RBCs), where it is rendered inactive until it is offloaded in the lungs (Kay et al., 1967; Gomez-Arroyo et al., 2011). Thus, the effects of MCT are seen primarily in the pulmonary vasculature mediated through a variety of only partially uncovered mechanisms including bone morphogenic protein receptor-2 (BMPR2) inhibition (Ramos et al., 2007). BMPR2 alterations are thought to be a primary contributor to the development and exacerbation of PH in patients (Teichert-Kuliszewska et al., 2006). There are several animal models of PH available. MCT was

chosen in this study for its inexpensive and reproducible nature, as well as the ability to replicate human pathology—namely PA remodeling, vascular lesions, and subsequent RV hypertrophy (Nogueira-Ferreira et al., 2015). Finally, as addressed above, this protocol entails a single muscle submaximal exercise condition, therefore further studies are warranted which target blood flow in skeletal and respiratory muscle during single-muscle versus whole-body exercise in order to understand the O_2-related mechanisms responsible for decreases in $\dot{V}O_2$max and exercise tolerance, etc. seen in patients.

Conclusions

These data support that: 1) Despite PO_2*is* kinetics parameters displaying no significant differences between groups, the lower PO_2*is* during seconds 10-26 of contractions may be related to the slowing of $\dot{V}O_2$ kinetics; and 2) NO has the capability to improve muscle oxygenation in PH, but the effects may be limited during exercise because compensatory mechanisms to increase oxygen delivery to the muscle may have already occurred under resting conditions. These findings may provide insight into potential small muscle mass exercise therapy to improve exercise tolerance in PH patients, as well as delineate potential mechanisms involved in the slowing of $\dot{V}O_2$ kinetics. It remains to be elucidated whether decrements in whole body exercise capacity result from peripheral vascular dysfunction, but our investigations herein suggest that they may play a role. These data provide direction for future studies investigating the distribution of blood flow during whole body exercise to determine the extent of oxygen delivery-related limitations in exercise tolerance in PH patients.

References

1. Akhavein, F., St.-Michel, E. J., Seifert, E., & Rohlicek, C. V. (2007). Decreased left ventricular function, myocarditis, and coronary arteriolar medial thickening following monocrotaline administration in adult rats. *Journal of Applied Physiology*, *103*(1), 287-295.).
2. Babu, A. S., Arena, R., Myers, J., Padmakumar, R., Maiya, A. G., Cahalin, L. P., ... & Lavie, C. J. (2016). Exercise intolerance in pulmonary hypertension: mechanism, evaluation and clinical implications. *Expert review of respiratory medicine*, *10*(9), 979-990.
3. Bailey, J. K., Kindig, C. A., Behnke, B. J., Musch, T. I., Schmid-Schoenbein, G. W., & Poole, D. C. (2000). Spinotrapezius muscle microcirculatory function: effects of surgical exteriorization. *American Journal of Physiology-Heart and Circulatory Physiology*, *279*(6), H3131-H3137.
4. Baker, J. S., McCormick, M. C., & Robergs, R. A. (2010). Interaction among skeletal muscle metabolic energy systems during intense exercise. *Journal of nutrition and metabolism*, *2010*.
5. Barbosa, P. B., Ferreira, E. M., Arakaki, J. S., Takara, L. S., Moura, J., Nascimento, R. B., Nery, L.E., & Neder, J. A. (2011). Kinetics of skeletal muscle O_2 delivery and utilization at the onset of heavy-intensity exercise in pulmonary arterial hypertension. *European journal of applied physiology*, *111*(8), 1851-1861.
6. Batt, J., Ahmed, S. S., Correa, J., Bain, A., & Granton, J. (2014). Skeletal muscle dysfunction in idiopathic pulmonary arterial hypertension. *American journal of respiratory cell and molecular biology*, *50*(1), 74-86.
7. Beaver, W. L., Wasserman, K.., & Whipp, B. J. (1986). Bicarbonate buffering of lactic acid generated during exercise. *Journal of Applied Physiology*, *60*(2), 472-478.
8. Benza, R. L., Miller, D. P., Barst, R. J., Badesch, D. B., Frost, A. E., & McGoon, M. D. (2012). An evaluation of long-term survival from time of diagnosis in pulmonary arterial hypertension from the REVEAL Registry. *Chest*, *142*(2), 448-456.

9. Bogaard, H. J., Abe, K., Noordegraaf, A. V., & Voelkel, N. F. (2009). The right ventricle under pressure: cellular and molecular mechanisms of right-heart failure in pulmonary hypertension. *Chest*, *135*(3), 794-804.
10. Borghi-Silva, A., Oliveira, C. C., Carrascosa, C., Maia, J., Berton, D. C., Queiroga, F., Ferreira, E.M., Almerida, D.R., Nery, L.E., & Neder, J. A. (2008). Respiratory muscle unloading improves leg muscle oxygenation during exercise in patients with COPD. *Thorax*, *63*(10), 910-915.
11. Brown, M. B., Chingombe, T. J., Zinn, A. B., Reddy, J. G., Novack, R. A., Cooney, S. A., Fisher, A.J., Presson, R.G., Lahm, T., & Petrache, I. (2015). Novel assessment of haemodynamic kinetics with acute exercise in a rat model of pulmonary arterial hypertension. *Experimental physiology*, *100*(6), 742-754.
12. Brown, M. B., Neves, E., Long, G., Graber, J., Gladish, B., Wiseman, A., Owens, M., Fisher, A.J., Presson, R.G., Petrache, I., & Kline, J. (2017). High-intensity interval training, but not continuous training, reverses right ventricular hypertrophy and dysfunction in a rat model of pulmonary hypertension. *American Journal of Physiology-Regulatory, Integrative and Comparative Physiology*, *312*(2), R197-R210.
13. Budhiraja, R., Tuder, R. M., & Hassoun, P. M. (2004). Endothelial dysfunction in pulmonary hypertension. *Circulation*, *109*(2), 159-165.
14. Cella, G., Bellotto, F., Tona, F., Sbarai, A., Mazzaro, G., Motta, G., & Fareed, J. (2001). Plasma markers of endothelial dysfunction in pulmonary hypertension. *Chest*, *120*(4), 1226-1230.
15. Chan, S. Y., & Rubin, L. J. (2017). Metabolic dysfunction in pulmonary hypertension: from basic science to clinical practice. *European Respiratory Review*, *26*(146).
16. Chesney, C. F., Allen, J. R., & Hsu, I. C. (1974). Right ventricular hypertrophy in monocrotaline pyrrole treated rats. *Experimental and molecular pathology*, *20*(2), 257-268.
17. Christman, B. W., McPherson, C. D., Newman, J. H., King, G. A., Bernard, G. R., Groves, B. M., & Loyd, J. E. (1992). An imbalance between the excretion of thromboxane and prostacyclin metabolites in pulmonary hypertension. *New England Journal of Medicine*, *327*(2), 70-75.

18. Cote, C. G., Yu, F. S., Zulueta, J. J., Vosatka, R. J., & Hassoun, P. M. (1996). Regulation of intracellular xanthine oxidase by endothelial-derived nitric oxide. *American Journal of Physiology-Lung Cellular and Molecular Physiology*, *271*(5), L869-L874.
19. Craig, J. C., Colburn, T. D., Caldwell, J. T., Hirai, D. M., Tabuchi, A., Baumfalk, D. R., Behnke, B.J., Ade, C.J., Musch, T.I., & Poole, D. C. (2019a). Central and peripheral factors mechanistically linked to exercise intolerance in heart failure with reduced ejection fraction. *American Journal of Physiology-Heart and Circulatory Physiology*.
20. Craig, J. C., Colburn, T. D., Hirai, D. M., Musch, T. I., & Poole, D. C. (2019b). Sexual dimorphism in the control of skeletal muscle interstitial PO_2 of heart failure rats: effects of dietary nitrate supplementation. *Journal of Applied Physiology*, *126*(5), 1184-1192.
21. D'Alonzo, G. E., Barst, R. J., Ayres, S. M., Bergofsky, E. H., Brundage, B. H., Detre, K. M., Fishman, A.P., Goldring, R.M., Groves, B.M., Kernis, J.T. & Levy, P. S. (1991). Survival in patients with primary pulmonary hypertension: results from a national prospective registry. *Annals of internal medicine*, *115*(5), 343-349.
22. Dawson, C. A. (1984). Role of pulmonary vasomotion in physiology of the lung. *Physiological reviews*, *64*(2), 544-616
23. de Man, F. S., Handoko, M. L., Groepenhoff, H., Van't Hul, A. J., Abbink, J., Koppers, R. J. H., Grotjohan, H.P., Twisk, J.W.R., Bogaard, H.J., Boonstra, A., & Postmus, P. E. (2009). Effects of exercise training in patients with idiopathic pulmonary arterial hypertension. *European Respiratory Journal*, *34*(3), 669-675.
24. Delp, M. D., & Duan, C. (1996). Composition and size of type I, IIA, IID/X, and IIB fibers and citrate synthase activity of rat muscle. *Journal of applied physiology*, *80*(1), 261-270.
25. Dimopoulos, S., Tzanis, G., Manetos, C., Tasoulis, A., Mpouchla, A., Tseliou, E., Vasileiadis, I., Diakos, N., Terrovitis, J., & Nanas, S. (2013). Peripheral muscle microcirculatory alterations in patients with pulmonary arterial hypertension: a pilot study. *Respiratory care*, *58*(12), 2134-2141.

26. Esposito, F., Reese, V., Shabetai, R., Wagner, P. D., & Richardson, R. S. (2011). Isolated quadriceps training increases maximal exercise capacity in chronic heart failure: the role of skeletal muscle convective and diffusive oxygen transport. *Journal of the American College of Cardiology*, *58*(13), 1353-1362.
27. Esipova, T. V., Karagodov, A., Miller, J., Wilson, D. F., Busch, T. M., & Vinogradov, S. A. (2011). Two new "protected" oxyphors for biological oximetry: properties and application in tumor imaging. *Analytical chemistry*, *83*(22), 8756–8765.
28. Farber, H. W., Miller, D. P., Poms, A. D., Badesch, D. B., Frost, A. E., Muros-Le Rouzic, E., Romero, A.J., Benton, W.W., Elliott, C.G., McGoon, M.D. & Benza, R. L. (2015). Five-year outcomes of patients enrolled in the REVEAL Registry. *Chest*, *148*(4), 1043-1054.
29. Fowler, R. M., Jenkins, S. C., Maiorana, A. J., Gain, K. R., O'Driscoll, G., & Gabbay, E. (2011). Measurement properties of the 6-min walk test in individuals with exercise-induced pulmonary arterial hypertension. *Internal medicine journal*, *41*(9), 679-687.
30. Fowler, R. M., Gain, K. R., & Gabbay, E. (2012). Exercise intolerance in pulmonary arterial hypertension. *Pulmonary medicine*, *2012*.
31. Fulton, R. M., Hutchinson, E. C., & Jones, A. M. (1952). Ventricular weight in cardiac hypertrophy. *British heart journal*, *14*(3), 413–420.
32. Giaid, A., Yanagisawa, M., Langleben, D., Michel, R. P., Levy, R., Shennib, H., Kimura, S., Masaki, T., Duguid, W.P. & Stewart, D. J. (1993). Expression of endothelin-1 in the lungs of patients with pulmonary hypertension. *New England Journal of Medicine*, *328*(24), 1732-1739.
33. Giaid, A., & Saleh, D. (1995). Reduced expression of endothelial nitric oxide synthase in the lungs of patients with pulmonary hypertension. *New England Journal of Medicine*, *333*(4), 214-221.
34. Gomez-Arroyo, J. G., Farkas, L., Alhussaini, A. A., Farkas, D., Kraskauskas, D., Voelkel, N. F., & Bogaard, H. J. (2011). The monocrotaline model of pulmonary hypertension in perspective. *American Journal of Physiology-Lung Cellular and Molecular Physiology*, *302*(4), L363-L369.
35. Grünig, E., Ehlken, N., Ghofrani, A., Staehler, G., Meyer, F. J., Juenger, J., Opitz, C.F., Klose, H., Wilkens, H., Rosenkranz, S., & Olschewski, H. (2011). Effect of

exercise and respiratory training on clinical progression and survival in patients with severe chronic pulmonary hypertension. *Respiration*, *81*(5), 394-401.

36. Guignabert, C., & Dorfmüller, P. (2017, October). Pathology and pathobiology of pulmonary hypertension. In *Seminars in respiratory and critical care medicine* (Vol. 38, No. 05, pp. 571-584). Thieme Medical Publishers.
37. Harms, C. A., Babcock, M. A., McClaran, S. R., Pegelow, D. F., Nickele, G. A., Nelson, W. B., & Dempsey, J. A. (1997). Respiratory muscle work compromises leg blood flow during maximal exercise. *Journal of applied physiology*, *82*(5), 1573-1583.
38. Hassoun, P. M., Yu, F. S., Cote, C. G., Zulueta, J. J., Sawhney, R., Skinner, K. A., Skinner, H.B., Parks, D.A. & Lanzillo, J. J. (1998). Upregulation of xanthine oxidase by lipopolysaccharide, interleukin-1, and hypoxia: role in acute lung injury. *American Journal of Respiratory and Critical Care Medicine*, *158*(1), 299-305.
39. Hirai, D. M., Craig, J. C., Colburn, T. D., Eshima, H., Kano, Y., Sexton, W. L., Musch, T.I., & Poole, D. C. (2018). Skeletal muscle microvascular and interstitial from rest to contractions. *The Journal of physiology*, *596*(5), 869-883.
40. Hoeper, M. M., Pletz, M. W., Golpon, H., & Welte, T. (2007). Prognostic value of blood gas analyses in patients with idiopathic pulmonary arterial hypertension. *European Respiratory Journal*, *29*(5), 944-950.
41. Hogan, M. C., Arthur, P. G., Bebout, D. E., Hochachka, P. W., & Wagner, P. D. (1992). Role of O_2 in regulating tissue respiration in dog muscle working in situ. *Journal of Applied Physiology*, *73*(2), 728-736.
42. Hu, H., & Sachs, F. (1997). Stretch-activated ion channels in the heart. *Journal of molecular and cellular cardiology*, *29*(6), 1511-1523.
43. Humbert, M., Monti, G., Brenot, F., Sitbon, O., Portier, A., Grangeot-Keros, L., Duroux, P., Galanaud, P., Simonneau, G. & Emilie, D. (1995). Increased interleukin-1 and interleukin-6 serum concentrations in severe primary pulmonary hypertension. *American journal of respiratory and critical care medicine*, *151*(5), 1628-1631.
44. Jones, J. E., Mendes, L., Rudd, M. A., Russo, G., Loscalzo, J., & Zhang, Y. Y. (2002). Serial noninvasive assessment of progressive pulmonary hypertension in a rat

model. *American Journal of Physiology-Heart and Circulatory Physiology*, *283*(1), H364-H371.

45. Kajiya, M., Hirota, M., Inai, Y., Kiyooka, T., Morimoto, T., Iwasaki, T., Endo, K., Mohri, S., Shimizu, J., Yada, T. & Ogasawara, Y. (2007). Impaired NO-mediated vasodilation with increased superoxide but robust EDHF function in right ventricular arterial microvessels of pulmonary hypertensive rats. *American Journal of Physiology-Heart and Circulatory Physiology*, *292*(6), H2737-H2744.
46. Kato, Y., Iwase, M., Kanazawa, H., Kawata, N., Yoshimori, Y., Hashimoto, K., Yokoi, T., Noda, A., Takagi, K., Koike, Y., & Nishizawa, T. (2003). Progressive development of pulmonary hypertension leading to right ventricular hypertrophy assessed by echocardiography in rats. *Experimental animals*, *52*(4), 285-294.
47. Kay, J. M., Harris, P., & Heath, D. (1967). Pulmonary hypertension produced in rats by ingestion of Crotalaria spectabilis seeds. *Thorax*, *22*(2), 176-179.
48. Kitabatake, A., Inoue, M., Asao, M., Masuyama, T., Tanouchi, J., Morita, T., ... & Abe, H. (1983). Noninvasive evaluation of pulmonary hypertension by a pulsed Doppler technique. *Circulation*, *68*(2), 302-309.
49. Klinger, J. R., Abman, S. H., & Gladwin, M. T. (2013). Nitric oxide deficiency and endothelial dysfunction in pulmonary arterial hypertension. *American journal of respiratory and critical care medicine*, *188*(6), 639-646.
50. Krasuski, R. A., Warner, J. J., Wang, A., Harrison, J. K., Tapson, V. F., & Bashore, T. M. (2000). Inhaled nitric oxide selectively dilates pulmonary vasculature in adult patients with pulmonary hypertension, irrespective of etiology. *Journal of the American College of Cardiology*, *36*(7), 2204-2211.
51. Lahm, T., Tuder, R. M., & Petrache, I. (2014). Progress in solving the sex hormone paradox in pulmonary hypertension. *American Journal of Physiology-Lung Cellular and Molecular Physiology*, *307*(1), L7-L26.
52. Lai, Y. L., Olson, J. W., & Gillespie, M. N. (1991). Ventilatory dysfunction precedes pulmonary vascular changes in monocrotaline-treated rats. *Journal of Applied Physiology*, *70*(2), 561-566.
53. Laughlin, M. H. (1999). Cardiovascular response to exercise. *Advances in physiology education*, *277*(6), S244.

54. Leek, B. T., Mudaliar, S. R., Henry, R., Mathieu-Costello, O., & Richardson, R. S. (2001). Effect of acute exercise on citrate synthase activity in untrained and trained human skeletal muscle. *American Journal of Physiology-Regulatory, Integrative and Comparative Physiology*, *280*(2), R441-R447.
55. Levy, P. T., Patel, M. D., Groh, G., Choudhry, S., Murphy, J., Holland, M. R., Hamvas, A., Grady, M.R., & Singh, G. K. (2016). Pulmonary artery acceleration time provides a reliable estimate of invasive pulmonary hemodynamics in children. *Journal of the American Society of Echocardiography*, *29*(11), 1056-1065.
56. Mainguy, V., Maltais, F., Saey, D., Gagnon, P., Martel, S., Simon, M., & Provencher, S. (2010). Peripheral muscle dysfunction in idiopathic pulmonary arterial hypertension. *Thorax*, *65*(2), 113-117.
57. Malenfant, S., Potus, F., Mainguy, V., Leblanc, E., Malenfant, M., Ribeiro, F., Saey, D., Maltais, F., Bonnet, S. & Provencher, S. (2015). Impaired skeletal muscle oxygenation and exercise tolerance in pulmonary hypertension. *Medicine & Science in Sports & Exercise*, *47*(11), 2273-2282.
58. Mann, D. L. (2004). Basic mechanisms of left ventricular remodeling: the contribution of wall stress. *Journal of cardiac failure*, *10*(6), S202-S206.
59. McCord, J. M. (1985). Oxygen-derived free radicals in postischemic tissue injury. *New England Journal of Medicine*, *312*(3), 159-163.
60. McGoon, M. D., Benza, R. L., Escribano-Subias, P., Jiang, X., Miller, D. P., Peacock, A. J., Pepke-Zaba, J.m Pulido, T., Rich, S., Rosenkranz, S., & Suissa, S. (2013). Pulmonary arterial hypertension: epidemiology and registries. *Journal of the American College of Cardiology*, *62*(25 Supplement), D51-D59.
61. Mereles D., Ehlken N., Kreuscher S., Ghofrani S., Hoeper M. M., Halank M., Meyer F. J., et al. (2006). Exercise and respiratory training improve exercise capacity and quality of life in patients withs ever chronic pulmonary hypertension. *Circulation*, 114(14), 1482-1489
62. Meyer, F. J., Lossnitzer, D., Kristen, A. V., Schoene, A. M., Kübler, W., Katus, H. A., & Borst, M. M. (2005). Respiratory muscle dysfunction in idiopathic pulmonary arterial hypertension. *European Respiratory Journal*, *25*(1), 125-130.

63. Meyrick, B., Gamble, W., & Reid, L. (1980). Development of Crotalaria pulmonary hypertension: hemodynamic and structural study. *American Journal of Physiology-Heart and Circulatory Physiology*, *239*(5), H692-H702.
64. Michelakis, E. D., Gurtu, V., Webster, L., Barnes, G., Watson, G., Howard, L., Cupitt, J., Paterson, I., Thompson, R.B., Chow, K. & O'Regan, D. P. (2017). Inhibition of pyruvate dehydrogenase kinase improves pulmonary arterial hypertension in genetically susceptible patients. *Science Translational Medicine*, *9*(413).
65. Musch, T. I. (1993). Elevated diaphragmatic blood flow during submaximal exercise in rats with chronic heart failure. *American Journal of Physiology-Heart and Circulatory Physiology*, *265*(5), H1721-H1726.
66. Nogueira-Ferreira, R., Vitorino, R., Ferreira, R., & Henriques-Coelho, T. (2015). Exploring the monocrotaline animal model for the study of pulmonary arterial hypertension: a network approach. *Pulmonary pharmacology & therapeutics*, *35*, 8-16.
67. Olson, T. P., Joyner, M. J., Dietz, N. M., Eisenach, J. H., Curry, T. B., & Johnson, B. D. (2010). Effects of respiratory muscle work on blood flow distribution during exercise in heart failure. *The Journal of physiology*, *588*(13), 2487-2501.
68. Partovian, C., Adnot, S., Eddahibi, S., Teiger, E., Levame, M., Dreyfus, P., Raffestin, B. & Frelin, C. (1998). Heart and lung VEGF mRNA expression in rats with monocrotaline-or hypoxia-induced pulmonary hypertension. *American Journal of Physiology-Heart and Circulatory Physiology*, *275*(6), H1948-H1956.
69. Peled, N., Bendayan, D., Shitrit, D., Fox, B., Yehoshua, L., & Kramer, M. R. (2008). Peripheral endothelial dysfunction in patients with pulmonary arterial hypertension. *Respiratory medicine*, *102*(12), 1791-1796.
70. Peled, N., Shitrit, D., Fox, B. D., Shlomi, D., Amital, A., Bendayan, D., & Kramer, M. R. (2009). Peripheral arterial stiffness and endothelial dysfunction in idiopathic and scleroderma associated pulmonary arterial hypertension. *The Journal of rheumatology*, *36*(5), 970-975.
71. Pepke-Zaba, J., Higenbottam, T. W., Dinh-Xuan, A. T., Stone, D., & Wallwork, J. (1991). Inhaled nitric oxide as a cause of selective pulmonary vasodilatation in pulmonary hypertension. *The Lancet*, *338*(8776), 1173-1174.

72. Poole, D. C., Barstow, T. J., McDonough, P., & Jones, A. M. (2008). Control of oxygen uptake during exercise. *Medicine and science in sports and exercise*, *40*(3), 462-474.
73. Poole, D. C., Hirai, D. M., Copp, S. W., & Musch, T. I. (2011). Muscle oxygen transport and utilization in heart failure: implications for exercise (in) tolerance. *American Journal of Physiology-Heart and Circulatory Physiology*, *302*(5), H1050-H1063.
74. Potus, F., Malenfant, S., Graydon, C., Mainguy, V., Tremblay, È., Breuils-Bonnet, S., Ribeiro, F., Porlier, A., Maltais, F., Bonnet, S. & Provencher, S. (2014). Impaired angiogenesis and peripheral muscle microcirculation loss contribute to exercise intolerance in pulmonary arterial hypertension. *American journal of respiratory and critical care medicine*, *190*(3), 318-328.
75. Ramos, M. F., Lamé, M. W., Segall, H. J., & Wilson, D. W. (2008). Smad signaling in the rat model of monocrotaline pulmonary hypertension. *Toxicologic pathology*, *36*(2), 311-320.
76. Rich, S., Dantzker, D. R., Ayres, S. M., Bergofsky, E. H., Brundage, B. H., Detre, K. M., Fishman, A.P., Goldring, R.M., Groves B.M., Koerner, S.K., & Levy, P. C. (1987). Primary pulmonary hypertension: a national prospective study. *Annals of internal medicine*, *107*(2), 216-223.
77. Rogers, N. M., Ghimire, K., Calzada, M. J., & Isenberg, J. S. (2017). Matricellular protein thrombospondin-1 in pulmonary hypertension: multiple pathways to disease. *Cardiovascular research*, *113*(8), 858-868.
78. Rosenberg, H. C., & Rabinovitch, M. (1988). Endothelial injury and vascular reactivity in monocrotaline pulmonary hypertension. *American Journal of Physiology-Heart and Circulatory Physiology*, *255*(6), H1484-H1491.
79. Ryan, J. J., Marsboom, G., & Archer, S. L. (2013). Rodent models of group 1 pulmonary hypertension. In *Pharmacotherapy of pulmonary hypertension* (pp. 105-149). Springer, Berlin, Heidelberg.
80. Sano, M., Minamino, T., Toko, H., Miyauchi, H., Orimo, M., Qin, Y., Akazawa, H., Tateno, K., Kayama, Y., Harada, M. & Shimizu, I. (2007). p53-induced inhibition of

Hif-1 causes cardiac dysfunction during pressure overload. *Nature*, *446*(7134), 444-448.

81. Shafazand, S., Goldstein, M. K., Doyle, R. L., Hlatky, M. A., & Gould, M. K. (2004). Health-related quality of life in patients with pulmonary arterial hypertension. *Chest*, *126*(5), 1452-1459.
82. Simonneau, G., Montani, D., Celermajer, D. S., Denton, C. P., Gatzoulis, M. A., Krowka, M., Williams, P.G., & Souza, R. (2019). Haemodynamic definitions and updated clinical classification of pulmonary hypertension. *European Respiratory Journal*, *53*(1).
83. Sithamparanathan, S., Rocha, M. C., Parikh, J. D., Rygiel, K. A., Falkous, G., Grady, J. P., Hollingsworth, K.G., Trenell, M.I., Taylor, R.W., Turnbull, D.M., & Gorman, G. S. (2018). Skeletal muscle mitochondrial oxidative phosphorylation function in idiopathic pulmonary arterial hypertension: in vivo and in vitro study. *Pulmonary circulation*, *8*(2), 2045894018768290.
84. Stasch, J. P., Pacher, P., & Evgenov, O. V. (2011). Soluble guanylate cyclase as an emerging therapeutic target in cardiopulmonary disease. *Circulation*, *123*(20), 2263-2273.
85. Sun, X. G., Hansen, J. E., Oudiz, R. J., & Wasserman, K. (2001). Exercise pathophysiology in patients with primary pulmonary hypertension. *Circulation*, *104*(4), 429-435.
86. Sun, X. G., Hansen, J. E., Oudiz, R. J., & Wasserman, K. (2003). Pulmonary function in primary pulmonary hypertension. *Journal of the American College of Cardiology*, *41*(6), 1028-1035.
87. Teichert-Kuliszewska, K., Kutryk, M. J., Kuliszewski, M. A., Karoubi, G., Courtman, D. W., Zucco, L., Granton, J., & Stewart, D. J. (2006). Bone morphogenetic protein receptor-2 signaling promotes pulmonary arterial endothelial cell survival: implications for loss-of-function mutations in the pathogenesis of pulmonary hypertension. *Circulation research*, *98*(2), 209-217.
88. Tomanek, R. J. (1990). Response of the coronary vasculature to myocardial hypertrophy. *Journal of the American College of Cardiology*, *15*(3), 528-533.

89. Tozzi, C. A., Poiani, G. J., Harangozo, A. M., Boyd, C. D., & Riley, D. J. (1989). Pressure-induced connective tissue synthesis in pulmonary artery segments is dependent on intact endothelium. *The Journal of clinical investigation*, *84*(3), 1005-1012.
90. Tuder, R. M., Cool, C. D., Geraci, M. W., Wang, J., Abman, S. H., Wright, L., Badesch, D. & Voelkel, N. F. (1999). Prostacyclin synthase expression is decreased in lungs from patients with severe pulmonary hypertension. *American journal of respiratory and critical care medicine*, *159*(6), 1925-1932.
91. Velez-Roa, S., Ciarka, A., Najem, B., Vachiery, J. L., Naeije, R., & Van De Borne, P. (2004). Increased sympathetic nerve activity in pulmonary artery hypertension. *Circulation*, *110*(10), 1308-1312.
92. Vescovo, G., Ceconi, C., Bernocchi, P., Ferrari, R., Carraro, U., Ambrosio, G. B., & Dalla Libera, L. (1998). Skeletal muscle myosin heavy chain expression in rats with monocrotaline-induced cardiac hypertrophy and failure. Relation to blood flow and degree of muscle atrophy. *Cardiovascular research*, *39*(1), 233-241.
93. West, J. B. (2012). *Respiratory physiology: the essentials*. Lippincott Williams & Wilkins.
94. Wolff, B., Lodziewski, S., Bollmann, T., Opitz, C. F., & Ewert, R. (2007). Impaired peripheral endothelial function in severe idiopathic pulmonary hypertension correlates with the pulmonary vascular response to inhaled iloprost. *American heart journal*, *153*(6), 1088-e1.